Wiley
Journal of Chemistry
Volume 2026, Article ID 6491268, 27 pages
https://doi.org/10.1155/joch/6491268

WILEY

*Review Article*

# Transfer Hydrogenation: Advances in Manganese and Nickel Metal Catalysis

**James Kamau, George S. Nyamato, and Joanne Ogunah**

*Department of Physical Sciences, University of Embu, P.O. Box 6-60100, Embu, Kenya*

Correspondence should be addressed to George S. Nyamato; simba.george@embuni.ac.ke

Received 30 July 2025; Revised 17 November 2025; Accepted 24 December 2025

Academic Editor: Munmun Bardhan



Transfer hydrogenation (TH) of ketones, catalyzed by transition–metal complexes, produces alcohols, which are important building blocks in the pharmaceutical and fine chemical industries. For a long time, catalysts based on noble metals such as ruthenium, rhodium, and iridium have dominated the TH of ketones. However, due to limited availability, high price, and toxicity of these noble metals, there has been a push for their replacement with abundant, nonprecious, and biocompatible metals. In this respect, the reactions catalyzed by first-row transition metals, which are more abundant and benign, have attracted more and more attention. Thus, in this review, we provide a comprehensive overview of the advances made in the last decade, in the application of the first-row transition metals, manganese and nickel, in the hydrogenation of ketones. Special focus is given to ligand design and reaction conditions in influencing the catalytic activity, yield, and the nature of the product.

**Keywords:** chiral alcohols; ketones; manganese; nickel; transfer hydrogenation

## 1. Introduction

Transfer hydrogenation (TH) is an important pathway for the reduction of ketones to secondary alcohols, which are versatile building blocks in the industry [1]. For example, in the petroleum industry, TH is used in the conversion of furfural (FUR) to furfuryl alcohol (FOL), a corrosion inhibitor in oil and gas pipelines, as well as a solvent to extract sulfur compounds in petroleum refining [2]. In the food industry, TH is employed in synthesizing gamma-valerolactone (GVL), an organic compound that finds application in biomass pretreatment to enhance biomass conversion. Moreover, GVL is a food additive that is mainly used as a solvent, antioxidant, flavor booster, and preservative [3]. In the pharmaceutical industry, TH, being enantiospecific, finds application in the synthesis of compounds that contain stereocenters, which are very important for bioactivity [4].

TH involves the transfer of a proton and a hydride from a donor molecule to an unsaturated substrate [5]. H-donors influence product formation yields as well as the conversion ratio. A good H-donor must have a low oxidation potential to allow for the formation of a hydride under mild conditions and be loosely bonded to the catalytic center [6]. Before choosing the H-donor, parameters such as the catalyst to be used, operating conditions, the nature of the unsaturated group, and equipment should be considered [6]. The commonly used hydrogen sources are isopropanol, formic acid, formate esters, and Hantzsch esters (1,4-dihydropyridine dicarboxylates) [7, 8]. While donors like formats and alcohols remain prevalent, biomass-derived diboron compounds [9] and water [10] are attractive in TH since they contribute to green chemistry principles.

Whereas ketone reduction can also be achieved by direct hydrogenation, TH is preferred over direct hydrogenation due to its enhanced safety, ability to operate under mild reaction conditions, cost-effectiveness, and enantioselectivity [11]. Due to the mild reaction conditions, TH is highly tolerant to several functional groups, including ethers, esters, halides, nitriles, amino-, and nitro-groups [12]. Thus, the keto-group can be selectively reduced in the presence of other functional groups to a chiral alcohol.

The concept of TH was first demonstrated by Hans Meerwein and Wolfgang Ponndorf, and independently by Verley (MPV reduction) in 1925, when they used isopropanol as a donor and aluminum isopropoxide catalyst to reduce ketones [13]. In the 1960s, advancement was made with the introduction of transition metal (TM) catalysts, and since then, precious metals like Ir [14], Ru [15], Rh [16], and Pd [17] have reigned as catalysts in the asymmetric reduction of ketones. However, due to the unavailability, toxicity, and high cost of these metals, there has been a growing interest in the search for alternative metals [18, 19]. Recently, the focus has shifted to first-row TMs like Mn [20], Ni [21], Co [22], and Fe [23] due to their abundance, cost-effectiveness, and low affinity to hydride ions. Thus, this review summarizes the advances made on TH of ketones from 2015 up to today, focusing on Mn and Ni complexes, paying special consideration to different ligand designs and reaction conditions.

*1.1. Factors Affecting the TH of Ketones.* The conversion ratios and yield in TH of ketones are mainly influenced by the nature of the catalyst [24], the nature of the base [25], and the ketone to be reduced [26]. Since the number and amount of additives in a reaction are limiting factors, the amount of base is a concern [7, 27]. A large amount of base activates the catalyst but affects the tolerance to functional groups in ketone substrates [28]. The nature of the base used plays a significant role in catalytic transfer hydrogenation (CTH) [29]. Strong bases (KOH, NaOH, $^{t}$BuOK) lead to higher catalytic activities than mild bases ($K_2CO_3$, $Na_2CO_3$) [30]. The effect of the nature of the base is best illustrated by a study by Magubane et al. who reduced acetophenone (2 mmol) using Ni-based catalyst **1** (Figure 1) (0.02 mol (1.0 mol%)) and isopropanol (5 mL) H-donor for 48 h at 82°C with bases (0.4 M) KOH, NaOH, $Na_2CO_3$, and $^{t}$BuOK and obtained conversions of 95, 84, 55, and 97%, respectively [31].

The nature of donor atoms in the ligand [32], denticity [33], chirality, coordination geometry, and catalyst amount [34] influences the conversion and enantioselectivity. TM complexes find catalytic application in TH due to chirality induction, tuneability, high stability, and selectivity [35]. Moreover, it has been established that the nature of ligands on the metal complex affects both the percentage yield and enantiomeric conversion [36]. The type of donor ligands influences the catalytic activity based on the activation free energy and oxidation state. This is well demonstrated by Zhou et al., who utilized complexes **2a** and **2b** having Lewis base functional ligands with O-H and N-H functional groups (Figure 1) [37]. In the reduction of acetophenone using $^{i}$PrOH and $^{t}$BuOK, **2a** outperformed **2b**. This is because the Mn-O catalytic system undergoes deprotonation and proceeds through an aromatization/dearomatization mechanism, which requires high energy to activate, unlike Mn-N, which follows a classical bifunctional hydrogen transfer mechanism. The Mn-O intermediate is also unstable; hence, it undergoes irreversible decomposition, affecting its activity. The number of donor atoms in a ligand (denticity) also influences activity due to steric effects,

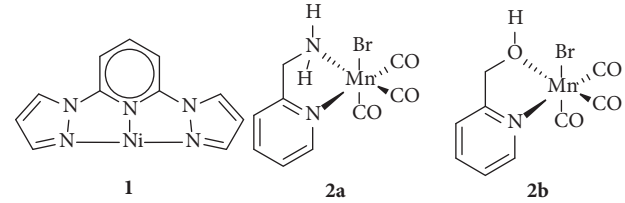


Figure 1: NNN, NN, and NO ligands coordinated to Ni and Mn metal centers.

electronic effects, stability, and coordination geometry [28, 38].

Catalyst loading is another parameter that dictates the conversion ratios [12]. Increasing catalyst loading has been found to enhance the percentage conversion, but only up to a certain point, after which it decreases [39]. This occurs due to aggregation, reductive demetallation, or oligomerization of the complex, which obstructs the active sites [40]. Moreover, the nature of substituents, bulkiness, and solubility in the reaction medium, and the presence of other functional groups in ketone substrates are also a concern [41]. Electron-donating groups (EDGs) in ketones lower the percentage yields, while electron-withdrawing groups (EWGs) stimulate the catalytic activity [42]. EDG leads to an increase in electron density on the metal center by increasing the electron-richness of the CO group, while EWG leads to a reduction [25].

*1.2. TH of Biomass-Derived Substrates.* The world is revolving, achieving net-zero $CO_2$ emissions and reducing the use of fossil fuels, which necessitates research on renewable sources [43]. Biomass, which is mainly composed of lignin, cellulose, and hemicellulose, has attracted attention due to its low cost, availability, cleanliness, abundant storage, and renewability. Biomass finds application in the production of biofuels and the production of carbon-based chemicals and materials (resins, fine chemicals, gasoline additives, medicine raw material, polymer nylon, materials, etc.). Biomass feedstock has a higher oxygen content than the value-added products like liquid biofuels or fuel additives [44]. CTH has been employed in the reduction of this oxygen-containing functional group, producing high-value products like GVL, FOL, DHMF, THFA, and 2-MF, among others [45].

Traditionally, TH of biomass has employed photocatalysts. These photocatalysts have disadvantages due to low migration efficiencies of photogenerated carriers, a wide band gap, and most require a precious metal co-catalyst, which makes them expensive [44]. Due to the high boiling points and easy decomposition in the vaporization process, most biomass-derived substrates are hydrogenated in the liquid phase [46]. The liquid hydrogen donors increase the intimate contact between the catalyst and the biomass substrate, hence increasing conversions. Most CTH of biomass-derived substrates has been utilizing nanocatalysts, which are prone to leaching and deposition at high temperature in the liquid phase, leading to catalyst deactivation [47].

Yunchao used Mn NPs in the TH of various biomass-derived substrates and obtained excellent conversions Table 1 [48]. Using HMF as the standard substrate, it was observed that conversions and yield increased with temperature and time. After the reaction was complete, the catalyst retained its crystal structure, showing no leaching, making it recyclable up to five times without loss in selectivity or activity. Low conversions of EL to GVL, even at elevated temperature and prolonged time, are attributed to the electron-donating ability of the alkyl group and the steric hindrance (entry 7). These reactions followed a direct hydrogen transfer mechanism, with nanoparticle size and N-doping influencing the catalyst activity. Manganese and nickel catalysts have been widely used in CTH of biomass-derived substrates [48–52].

*1.3. Mechanistic Pathways for TH.* CTH is a redox reaction where the hydrogen in the form of hydride is transferred from a donor (oxidized) to an acceptor (reduced) with the help of a catalyst [53]. Understanding the CTH mechanism helps in catalyst design, choice of donor and base, to increase conversions. CTH occurs either by the proton–electron transfer (PET) pathway or the hydrogen atom transfer (HAT) pathway [6, 54]. The PET pathway involves the dehydrogenation of a hydrogen donor on the catalyst sites and activation of the unsaturated group via absorption on the Lewis acid (LA) of the catalyst. Transfer of active hydrogen (hydride) follows this from the catalyst site to the unsaturated group. The HAT pathway, on the other hand, involves absorption and activation of both the hydrogen donor and the unsaturated group on LA sites of the catalyst, followed by the hydrogen transfer via the Meerwein–Ponndorf–Verley (MPV) mechanism [55]. The PET pathway occurs by either an outer-sphere mechanism or a metal–ligand cooperation (MLC) mechanism. Outer-sphere mechanism involves PET without the substrate directly bonding to the metal center, and it is commonly used for catalytic systems with a LA bifunctionality Scheme 1 [56].

The MLC mechanism is where the incoming substrate bonds with both the ligand backbone and the metal center, and it is commonly used for bifunctional catalysts with -N-H and –O-H moieties [57, 58]. In the outer-sphere mechanism, the donor and base interact with the catalyst, forming a bifunctional species [59]. The substrate forms a non-covalent bond (hydrogen bonding) with the metal complex [60]. The ligand-bound proton and metal-bound hydride are simultaneously transferred to the carbonyl group of the substrate [61]. The product then detaches from the catalyst, regenerating the bifunctional catalyst.

HAT pathway, also referred to as the inner-sphere mechanism, involves the formation of an alkoxide intermediate that undergoes hydride elimination to form metal hydride. The inner-sphere mechanism is experienced for complexes with vacant coordination sites [62]. This mechanism involves four key steps: catalyst activation, donor and substrate coordination, proton $H^+$ and hydride $H^-$ transfer, and catalyst regeneration (Scheme 2) [63].

With the help of a base, the catalyst is activated by generating vacant coordination sites [24]. The donor coordinates on the vacant sites where it undergoes β-hydride elimination, transferring the proton to the basic sites of the catalyst, and the hydride to the metal center [36]. This leads to the formation of metal–hydride species. The substrate then coordinates to the inner sphere of the metal. The hydride on the metal center migrates to the carbonyl carbon, leading to the formation of a metal–alkoxide intermediate [64]. The proton on the basic sites protonates these intermediates, leading to the formation of the alcohol [65]. The product then dissociates, leading to the formation of vacant sites ready to coordinate another substrate.

## 2. Manganese Complexes

The field of manganese complexes in the TH of ketones has seen significant advancements from 2015 to 2025. This period has been marked by the development of various manganese-based catalysts that demonstrate efficiency, selectivity, and the ability to operate under mild conditions. Manganese is the fourth most abundant TM in the Earth's crust, making it a more sustainable and economically viable alternative to precious metals like ruthenium, rhodium, and iridium. The use of manganese complexes allows for the development of catalytic systems that are less expensive and more accessible for large-scale applications.

Recent studies have begun to unravel the unique mechanisms by which manganese complexes catalyze TH reactions. The involvement of specific hydride transfer mechanisms, as elucidated by Demmans et al., indicates that manganese complexes can access unique transition states that may not be available to precious metal catalysts [28]. This insight into the mechanistic pathways enhances the understanding of manganese catalysis and opens avenues for further optimization of these systems.

*2.1. Bidentate Manganese Complexes.* Over the last decade, several Mn complexes chelated by bidentate ligands, with different donor atoms, have been developed and used for TH. For example, Mn complexes **3–6**, bearing bidentate aminomethylpyridine ligands, were used for THK at room temperature with catalyst loading below 0.1 mol% and produced TON of up to 2000 and TOF up to 3600 $h^{-1}$ (Figure 2) [67]. Complexes **3** and **4** were more active than **5** and **6,** underscoring the significance of the choice of ligands in TH and revealing that NH moieties are crucial for hydrogen transfer. In another related TH study, the significant role played by NH moieties in ligand systems was brought out by Ding and coworkers when they synthesized Mn complexes in situ using chiral diamine ligands to catalyze the reduction of sterically hindered ketones, affording up to 90% ee [66]. These ligands included aminomethylpyridine **L1**, N-methyl aminomethylpyridine **L2**, N,N-di-methyl amino-methylpyridine **L3**, 2-amino-pyridine **L4**, 1,2-diaminobenzene **L5**, 1,8-diamino-naphtalene **L6**, and (1R,2R)-N,N′-dimethyl-1,2-diphenylethane-1,2-diamine **L7** (Figure 2).

Table 1: TH of biomass-derived substrates using MnO@C-N[a].

| Entry | Substrate | Product | Temp °C | T (h) | % con | % yield |
|---|---|---|---|---|---|---|
| 1 | 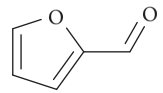 | 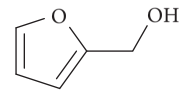 | 160 | 12 | 100 | 99 |
| 2 | 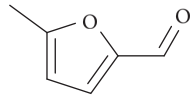 | 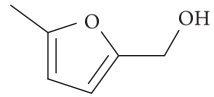 | 160 | 9 | 99 | 99 |
| 3 | 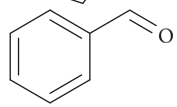 | 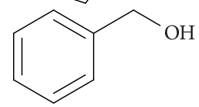 | 160 | 12 | 98 | 99 |
| 4 | 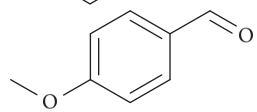 | 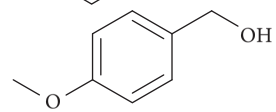 | 160 | 21 | 97 | 98 |
| 5 | 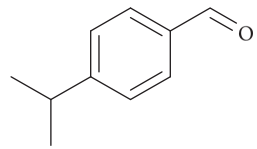 | 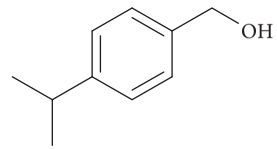 | 160 | 21 | 97 | 98 |
| 6 | 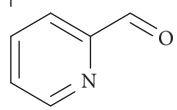 | 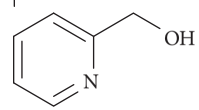 | 160 | 12 | 100 | 96 |
| 7 | 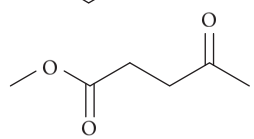 | 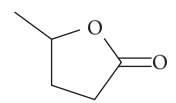 | 200 | 30 | 43 | 99 |

[a]Conditions: 0.1 g catalyst, 0.26 g substrate, 20 ML IPA.

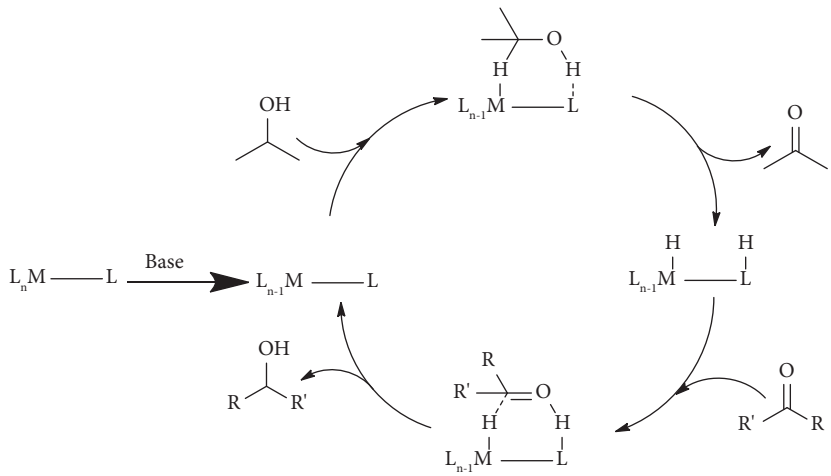

Scheme 1: Outer-sphere reaction mechanism [56].

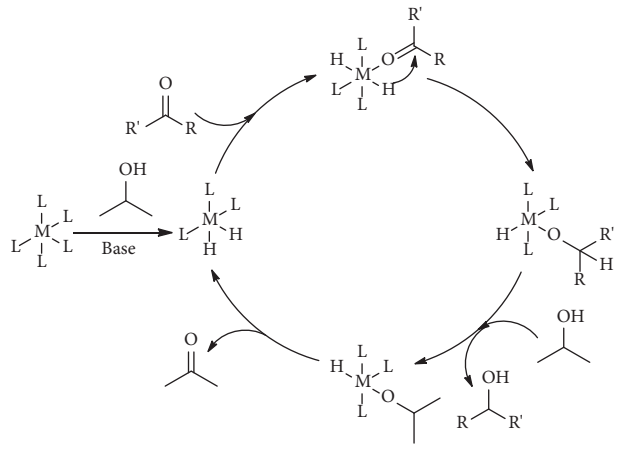

Scheme 2: Inner-sphere reaction mechanism [63].

**L1** and **L2** showed almost full conversion of 97% and 96%, respectively, of acetophenone to the corresponding alcohol after 1 h due to the NH moieties of the ligands. **L3** was almost inactive (6% conversion), while the aromatic amines ligands **L4**-**L6** (0%, 3%, and 0% conversions, respectively) did not promote the hydrogen transfer. Among these ligands, (1R,2R)-N,N′-dimethyl-1,2-diphenylethane-1,2-diamine **L7** showed the best activity as seen in Scheme 3. This approach was economically favorable since both the metal precursor (manganese pentacarbonyl bromide) and the ligand were cheap.

The effect of the N-H group on catalytic TH has also been reported by Ganguli, who utilized complexes **7(a-e)** and **8** bearing N-H and benzimidazole fragments in reducing ketones (Figure 3) [68]. Among these complexes, **7a** showed high activity (98% yields). Complex **7b** gave 52% yield, and complexes **7c** and **7d** showed moderate reactivity, while complex **7e** showed poor results. This indicates the significance of the N-H group in the ligand, which helps in the MLC mechanism. Complex **8** showed lower activities compared to **7a**, and this is caused by the difficulty in dissociation of the amine side arm or CO from the center to generate a vacant site, required for the formation of active Mn-H species. From the DFT calculations, it is noted that the reaction followed a concerted outer-sphere mechanism.

Besides the N-H group, the OH group also acts as a proton donor in TH reactions and its influence was reported by Dubey and coworkers who used bipyramid-based Mn complexes in their investigations (**9(a, b), 10(a, b), 11(a, B)**) and observed the highest activity from the complexes with the OH group (Figure 4) [69]. The position of the OH group did not affect the conversion, as complex **10a** showed similar activity with complex **9b**. Complex **10a** showed no activity while complexes **10b**, **11a,** and **11b** showed less activity, as evidenced in Table 2. Thus, the presence of the OH group, which is easily deprotonated under basic conditions, is crucial in enhancing activity, consistent with the findings of Martínez-Ferraté et al. [70]. The deuterium study revealed that the reaction followed the monohydride pathway.

Interestingly, the effect of steric bulk in TH was studied in another report for the chiral complexes **12, 13,** and **14** bearing aminobenzimidazole ligands (Figure 5) [71]. Generally, these complexes exhibited high activity and selectivity in the reduction of ketones. For example, complex **12a** afforded 95% yield with 65% ee in the reduction of

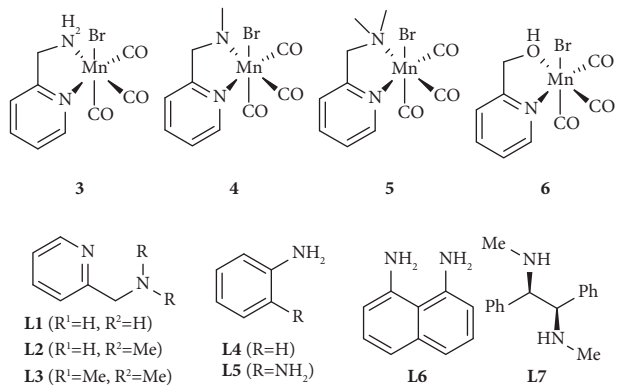


Figure 2: Aminomethylpyridine-chelated Mn complexes (**3–6)** and chiral diamine ligands with NH moieties (**L1**–**L7**) [66].

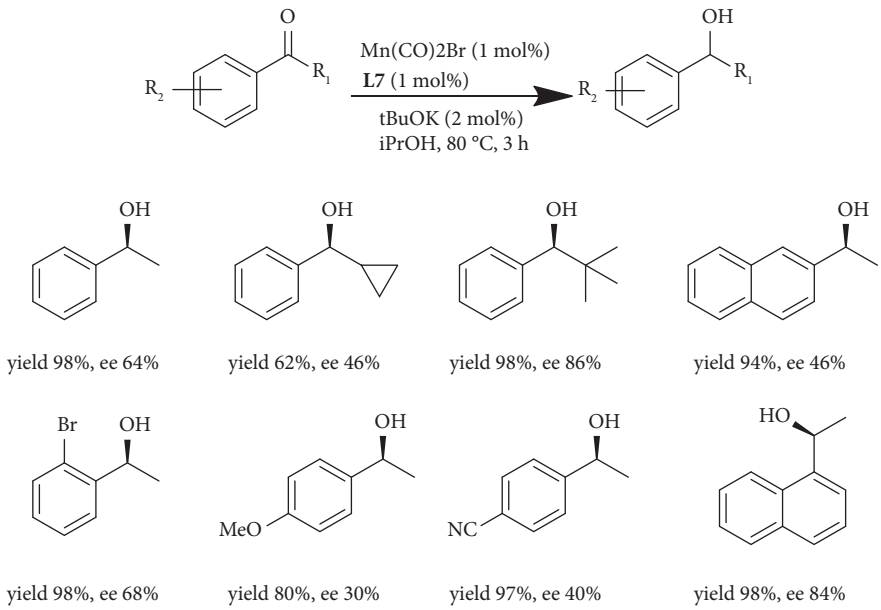


Scheme 3: Conversions in TH of aromatic ketones catalyzed by $[Mn(CO)_2Br]$ ligated with **L7** [66].

acetophenone using iPrOH in the presence of $^{t}$BuOK at 80°C after 20 min. The sterically hindered complex **12c** gave similar results as **12a** (88% yield and 66% ee), while less bulky complex **12b** afforded lower ee (97% yield and 42% ee). Complex **13a** gave high conversion with moderate ee (95% yield and 48% ee), while proline-based complex **13b** showed high ee (90% yield and 82% ee). Complexes **13c** and **13d** bearing aromatic ligands had moderate ee (82% and 76% ee, respectively), but complex **14** did not show any activity. The inactivity of complex **14** can be attributed to the steric effect since the phenyl group obstructs the approach of the substrate to the active site. Most importantly, complex **13b** was also used to reduce 6-dichloro-3-fluoroacetophenone to chiral alcohol (intermediate for crizotinib) with 92% ee and 90% yield. From the DFT calculations, it is noted that the π–π stacking interactions between the complex and the ketone play a key role.

In yet another interesting report, Mn artificial metalloenzymes (ArMs) were synthesized by reacting Mn complex **15** with S112 and K121 to form Mn-sav S112Y and Mn-sav K121M, respectively [72]. The synthesis was possible due to the bio-compatibility and low toxicity of Mn. Streptavidin possesses a high affinity for biotin, making it compatible with Mn. These ArMs were then utilized to reduce acetophenone, where Mn-sav K121M gave 46% yield and 80% ee, while Mn-sav S112Y gave 43% yield and 81% ee, as shown in Scheme 4. They were also used to reduce other ketones and high yields of up to 99%, with 85%–98% ee obtained.

Kumah and coworkers developed a dinuclear Mn(II) complexes **16-19** with carboxamide ligands, which easily fine-tunes steric and electronic parameters of the complexes (Figure 6) [73]. From single-crystal X-ray crystallographic analysis of these complexes, a distorted octahedral geometry is observed around the metal center. In TH of acetophenone using iPrOH at 82°C with 0.015 mol% catalyst and tBuOK base, complex **16** gave the highest yield compared to **17** (Table 3). The difference in activity is brought by the electronic properties of these complexes. For complex **16,** the dipicolinamide moieties are at para positions, increasing the electrophilicity of the metal center, unlike that of complex

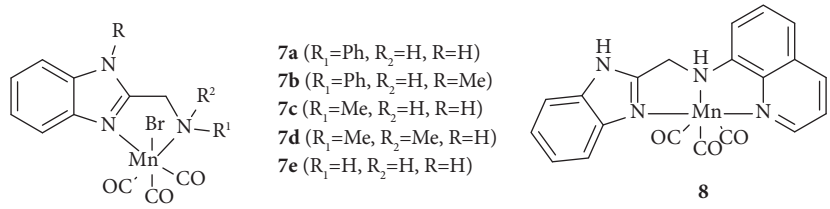


Figure 3: NN and NNN-Mn complexes bearing NH moieties.

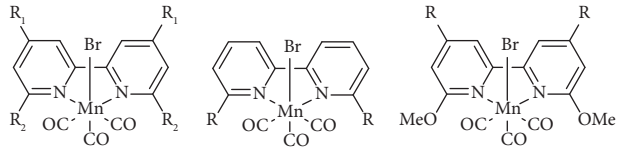


Figure 4: Bipyramid-based Mn complexes showing the influence of the OH group on catalytic activity.

Table 2: TH of acetophenone catalyzed by bipyramid-based Mn complexes **9–11** [69].

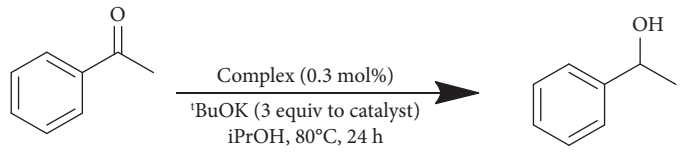


| Complex | % conversion | % yield |
|---|---|---|
| **9a** | > 99 | 94 |
| **9b** | > 99 | 94 |
| **10a** | < 1 | n.d |
| **10b** | 70 | 65 |
| **11a** | 40 | 28 |
| **11b** | 60 | 52 |

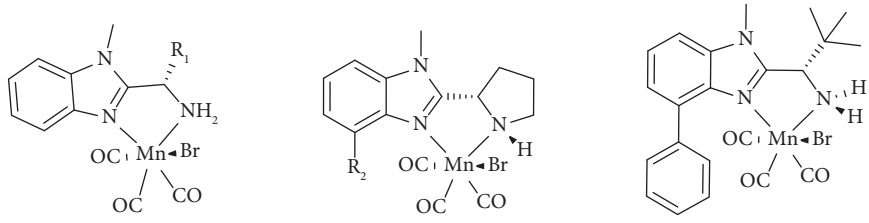


Figure 5: Mn complexes bearing aminobenzimidazole ligands.

**17**, which are at ortho positions. The higher thermal stability of complex **16** compared to **17** influences catalytic activity. Complexes **18** and **19** also gave moderate activity. Upon investigating different donors, it is noted that secondary alcohol donors gave good results compared to primary alcohol donors (entries 5–9). This is because secondary alcohols possess a sigma-inductive effect, and primary alcohols form aldehydes, which can poison the catalyst since they undergo alpha-alkylation under basic conditions [39]. Methanol and $HCOONa/H_2O$ did not give traceable results.

*2.2. Tridentate Mn Complexes.* Manganese complexes chelated by tridentate ligands have also been explored for TH with good outcomes. Perez and coworkers, for example, investigated Mn-N,N,N-pincer complexes **20–24**

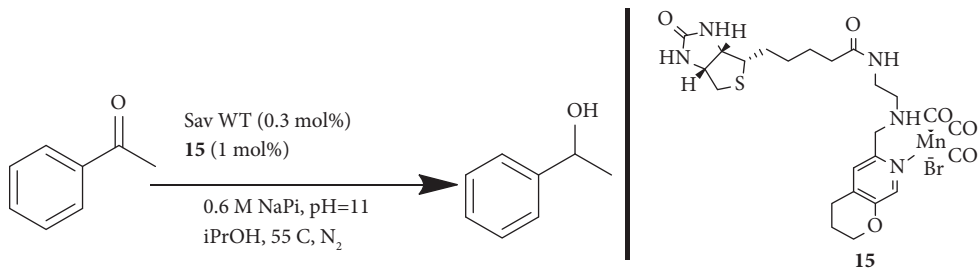


Scheme 4: TH of acetophenone catalyzed by ArMs complex **15** [72].

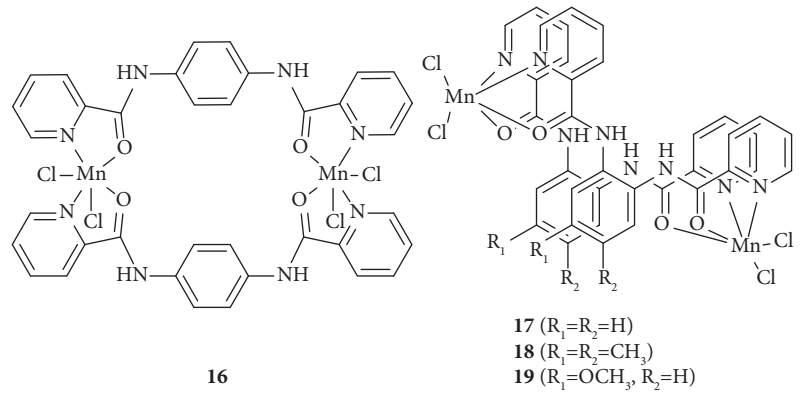


Figure 6: Dinuclear Mn(II) complexes with carboxamide ligands.

Table 3: TH of acetophenone catalyzed by dinuclear Mn(II) complexes **16–19** [73].

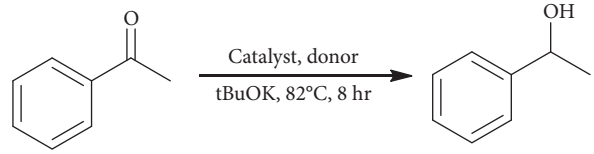


| Entry | Catalyst | Donor | Yield % | TON |
|---|---|---|---|---|
| 1 | **16** | i-Propanol | 79 | 2633 |
| 2 | **17** | i-Propanol | 68 | 2267 |
| 3 | **18** | i-Propanol | 61 | 2033 |
| 4 | **19** | i-Propanol | 70 | 2333 |
| 5 | **16** | 2-butanol | 82 | 410 |
| 6 | **16** | n-Propanol | 68 | 340 |
| 7 | **16** | HCOONa/Water | Trace | Trace |
| 8 | **17** | Methanol | Trace | Trace |
| 9 | **17** | Ethanol | 30 | 150 |

as THK catalysts (Figure 7) [74]. Complexes **20, 22,** and **23** gave moderate to good yields. Complex **23** afforded the highest conversion (96%) compared with the other complexes in the reduction of acetophenone, and its better performance was attributed to catalyst stabilization by the tridentate amine ligand, which enhanced the activity. The complex **24a** (3 mol%) achieved a conversion of up to 96% in the reduction of acetophenone when isopropanol was used as the donor, together with $^{t}$BuOK base at 70°C for 24 h. Upon replacing the N-H moiety in **24a** with a methyl group (complex 2**4b**), the results did not change, suggesting that the N-H moiety is not mandatory for activation. The influence of ligand architecture was evident on the performance of complex **21,** with a pyridine backbone, which was very low due to steric effects. To gain insight into the effect of the nature of the ketone on TH performance, various acetophenone derivatives were investigated, and it was observed that halogen-containing substrates gave yields up to 99%. Besides, 1,4-diacetylbenzene was also reduced to the corresponding diol with 99% conversion and 72% yield. On the other hand, heteroaromatic ketones were reduced, although they required high catalyst loading to give excellent results. Furthermore, it was also noted that the reaction followed the monohydride mechanism, hence, could proceed through either an inner- or outer-sphere pathway.

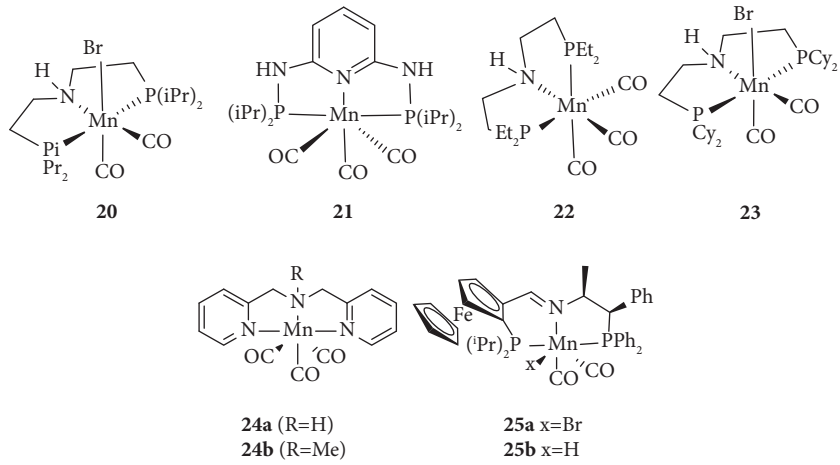


Figure 7: Mn-PNP and NNN-pincer complexes.

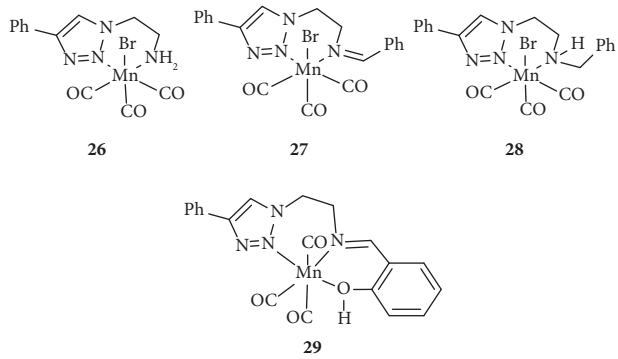


Figure 8: Mn complexes bearing amino-triazole ligands.

Similarly, Zirakzadeh and coworkers obtained impressive results for Mn complexes **25(a, b)** chelated by unsymmetrical chiral PNP' tridentate ligands (Figure 7) [63]. These catalysts showed high conversion of up to 96% and ee up to 86% (all the product configuration was found to be S), which can be accounted for by hydrogen bonding between the ligand and the oxygen atom of the substrate. Remarkably, complex **25b** was faster than **25a** since it reduced acetophenone for 2 h with a conversion of 95% and 86% ee, unlike **25a** with a conversion of 95% and 7% ee after 5 h. The high conversion in **25b** can be accounted for by the high lability of H compared to Br. Moreover, these complexes showed excellent results at room temperature, indicating an advancement from that of Perez et al. [74], which was not functional at room temperature.

In 2018, Martínez-Ferraté and coworkers studied Mn complexes **26**-**29** bearing amino-triazole ligands for TH catalysis using a wide range of ketones (Figure 8) [70]. Using complex **26** to investigate the optimum conditions, it was observed that with a catalyst loading of 3 mol%, high activity with 90% yield at 80°C after 20 h was obtained. It was further observed that upon decreasing the temperature to 60°C, the yield dropped to 52%, indicating that the reaction was temperature-dependent. Notably, complex **29** showed the lowest activity due to the presence of the phenol group in the coordination sphere. The phenol group can be easily deprotonated in the presence of a base to form a stable phenolate that prevents entry into the catalytic cycle. On the other hand, complex **28** bearing the amino moiety showed higher activity (up to 83% yield) than complex **27** bearing the imino moiety (only 15% yield). This is because the proton of the amino ligand is directly involved in the reduction step since the mechanism was through the outer sphere.

In yet another interesting report, TH of acetophenone using iPrOH was prepared by mixing $Mn(CO)_5Br$ metal precursor with aminophosphine ligands **L8**-**L17** by Karim and coworkers (Figure 9) [75]. For ligand **L8a,** the system was very active, as 80% conversion was obtained after 15 min at 80°C, but this system had poor selectivity (3% ee). The selectivity of this system was increased to 12% ee by reducing the reaction temperature to 30°C, but the reaction time increased to 19 h. From the results, as shown in Table 4, it is evident that steric hindrance, alkylation of the N atom, and chirality of the ligands influenced both selectivity and conversion. Since ligand **12b** proved to be the most effective, it was coordinated to a metal center to make complex **30,** which was obtained as a diastereomer.

Complex **30** afforded 75% ee and 96% conversion in the reduction of acetophenone at 30°C for 14 h, which is a good yield compared to the *in situ* system. This complex reduced a wide range of ketones, including ortho-substituted (2-

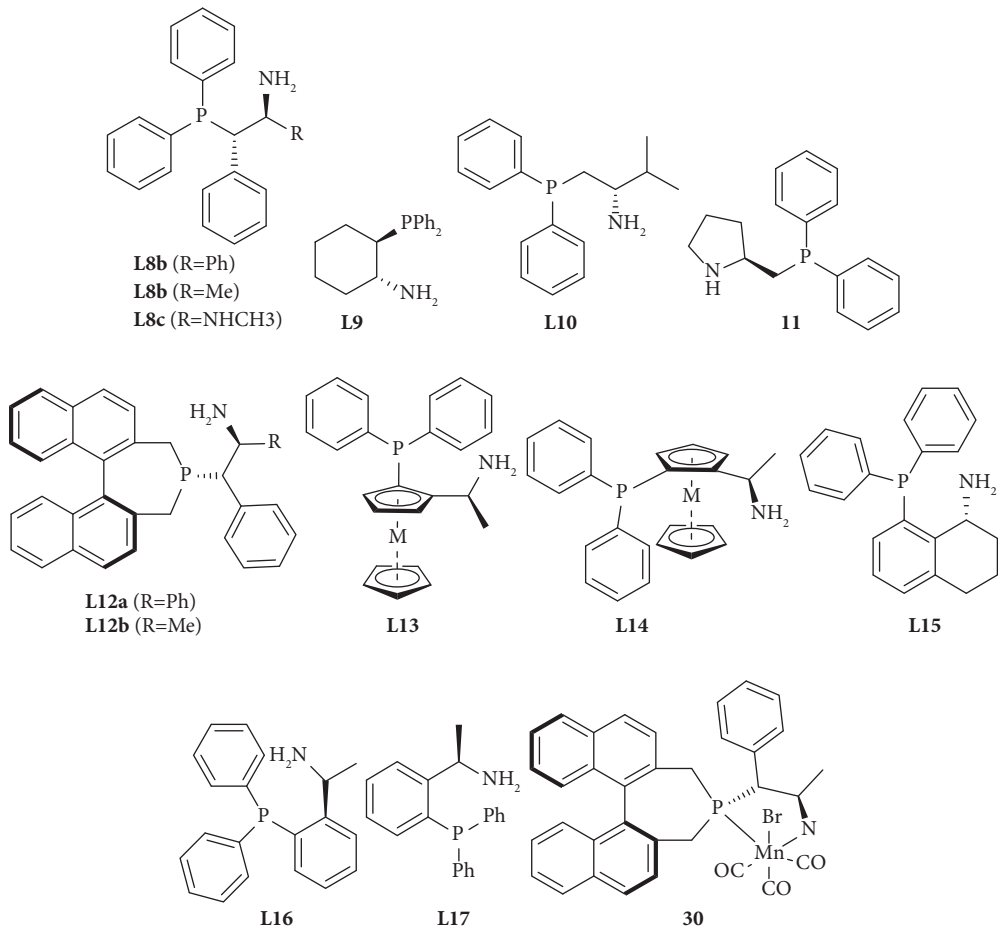


Figure 9: Aminophosphine ligands used in situ catalytic system with $Mn(CO)_5Br$ precursor by Karim and coworkers.

Table 4: Catalytic TH of acetophenone using the in situ catalytic systems with ligands **8–17** [75].

| Ligand | Temperature °C | V iPrOH | Time | Ee% | Conv % |
|---|---|---|---|---|---|
| **8a** | 80 | 8 | 15 | 3 (R) | 80 |
| **8a** | 80 | 8 | 45 | 2 (R) | 90 |
| **8a** | 30 | 20 | 19 | 12 (R) | 90 |
| **9** | 30 | 20 | 19 | 15 (S) | 97 |
| **8b** | 30 | 20 | 19 | 46 (R) | 96 |
| **10** | 30 | 20 | 19 | 11 (R) | 24 |
| **8c** | 30 | 20 | 19 | 65 (R) | 90 |
| **11** | 30 | 20 | 19 | 5 (S) | 97 |
| **12a** | 30 | 20 | 19 | 57 (R) | 96 |
| **12b** | 30 | 20 | 14 | 77 (R) | 95 |
| **12b** | 30 | 20 | 19 | 71 (R) | 95 |
| **13** | 30 | 20 | 19 | 20 (S) | 8 |
| **14** | 30 | 20 | 19 | 18 (R) | 10 |
| **15** | 30 | 20 | 19 | 25 (S) | 97 |
| **16** | 30 | 20 | 19 | 1 (R) | 97 |
| **17** | 30 | 20 | 19 | 2 (S) | 97 |

methylacetophenone—68% ee, 2-chloroacetophenone—72% ee), para-substituted (4-chloroacetophenone—64% ee, 4-methylacetophenone—77% ee), bulky-substituted (cyclopropyl(phenyl)methanone-73% ee), heteroaromatics (4-acetylpyridine-40% ee), polyaromatics (1-acetonaphthone-79% ee), and alkyl alkyl ketones (cyclohexyl methyl ketone—18% ee).

Interestingly, 1-(2-diphenylphosphino)ferrocenylethylamine also ligated with Mn in a tridentate fashion to form PNN pincer complex **31** (Figure 10) [32]. This complex

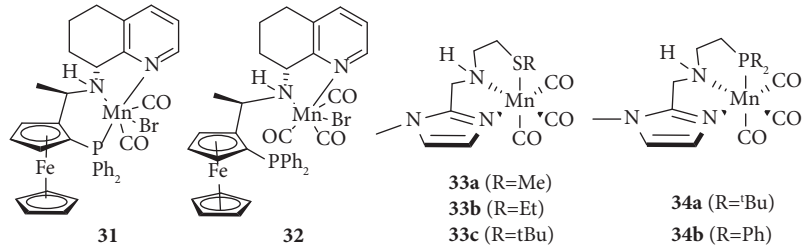


Figure 10: Air-stable PNN, NN, and NSS pincer complexes.

showed high ee excess due to π–π interactions and steric hindrance between the catalyst and substrate. The tridentate complex **31** proved to be more effective in THK (conversion of up to 99% with up to 99% ee) compared to the bidentate complex **32**. This is because complex **31** is much more stable due to high chelation strength and a better electronic and steric environment. The effect of the nature of the substituent of the ligand and hence electronic environment are further illustrated by the air-stable Mn complexes **33(a-c)** bearing NNS ligands (Figure 10) [12].

In the TH of acetophenone at room temperature, $^{t}$Bu-substituted complex **33c** showed the highest activity (76% conversion). In contrast, Me-substituted and Et-substituted complexes **33a** and **b** gave lower activities of 32% and 27% conversion, respectively. The difference is brought by the steric effects of the substituents on the S-donor atom. This is so because the formation of amido species likely occurred via loss of hemilabile S-donor rather than CO ligand; hence, loss of sterically hindered $^{t}$Bu-thioether in **33c** is more favored compared to Me- and Et-thioether in **33a** and **33c,** respectively. In addition, it was noted that at a higher temperature of 80°C, a high conversion of up to 96% was achieved in 20 min, which was accounted for by the ease of forming hydrido species at elevated temperature. It is noted that under the same conditions, complexes bearing NNS outshone NNP complexes **34a** and **b** (Figure 10). For less electron-donating NNS ligands, the formation of the amido group is more favorable than for more electron-donating PNN ligands.

Another related study involving PNN-based Mn pincer complexes **35-37** was recently reported, in which complex **35** was obtained by reacting $Mn(CO)_5Br$ and 2,6-{($PPh_2$) $CH_2N(Me)$ ($C_5H_3N$) ($C_2HN_3C_6H_5$)} at room temperature, while complexes **36** and **37** were obtained by reacting **35** with DCM in diethyl ether and $AgBF_4$ in DCM, respectively (Figure 11) [76]. The effect of the nature of the base on TH was explored using various bases, where it was observed that with KOH, complex **36** and $^{i}$PrOH donor yielded the highest conversion (99%) compared to $^{t}$BuOK, $K_2CO_3$, and NaOH, which gave moderate conversions, which is inconsistent with the order of base strength. Variation of alcohol donors to EtOH and MeOH led to reduced conversion to 15% for EtOH and no reaction for MeOH, which was attributed to the formation of $EtO^-$ or $MeO^-$ that poisons the catalyst, forming a stable and inactive carbonyl complex [6]. Among the three complexes, **36** showed the highest activity compared to **35** and **37** (96% and 95% conversions, respectively) due to the cationic nature of **35** and **37**. It was further proposed that the reaction starts by catalyst activation by the base and $^{i}$PrOH, forming a reactive intermediate which undergoes β-hydride elimination followed by hydride transfer via the outer-sphere mechanism.

*2.3. Tetradentate Mn Complexes.* Several Mn complexes for TH, bearing tetradentate ligands, have also been reported in the last decade. Notably, the PNN and PNNP complexes **38–40** exhibited temperature-dependent conversions of acetophenone using iPrOH donor (Figure 12) [28]. For example, **40** gave 99% conversion at 80°C and 56% conversion at 28°C. Under the same conditions, **38** and **39** were less active, as no conversions were observed at 28°C, with only 3% conversion observed for **38** at 80°C. Generally, complex **40** was found to be more active due to the presence of a halide (bromo ligand), which is labilized by a base to form an amido–Mn complex and potassium bromide, but in **38** and **39,** there is no formation of an open system. The amido Mn intermediate reacts with iPrOH, transferring the proton and hydride through the outer-sphere mechanism, forming the NH hydride intermediate. Notably, a little amount of base is needed with this mechanism, making it attractive for the reduction of ketones bearing base-sensitive functional groups, such as the reduction of p-acetyl benzoate ethyl ester that proceeds without a transesterification product (99% conversion with 31% ee within 2 h).

The effect of ligand architecture on TH has also been reported in a study involving a combination of $[MnBr(CO)_5]$ and chiral macrocyclic ligand **L18–23** (Figure 13) [77]. Using **L24** together with $[MnBr(CO)_5]$, acetophenone was reduced to optically active 1-phenylethanol by iPrOH with KOH base after 2 h at 75°C (99% conversion and 21% ee), while **L10** afforded a conversion of 42% and 71% ee.

Polydentate $P_3N_4$-type ligands **L20** and **L21** displayed good activity and moderate enantioselectivity (conversion 87% and 65% ee, conversion 66% and 67% ee, respectively). Similar results were obtained for the macrocyclic ligands **L22** and **L23,** although with different enantioselectivity (99% conversion, 81% ee, and 69% ee, respectively). The high activities of these ligands can be accounted for by steric hindrance rather than the N-H group, as in many $P_xN_y$-type ligands. Interestingly, under similar conditions, $[MnCl_2]$/**L23** was catalytically inactive, while $[Mn_2(CO)_{10}]$/**L23** gave poor conversion and low enantioselectivity (23% conversion and 47% ee). It is also noted that these complexes were base and temperature-dependent.

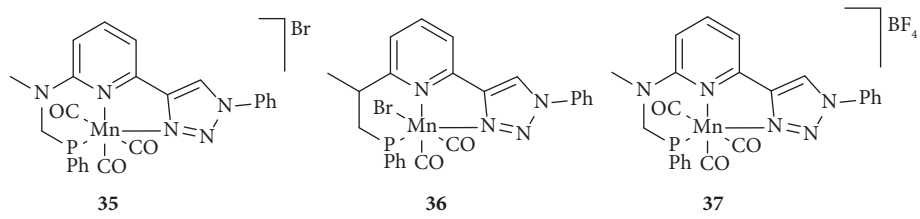

35 36 37

Figure 11: Mn complexes bearing triazolyl-pyridine-based phosphine ligands.

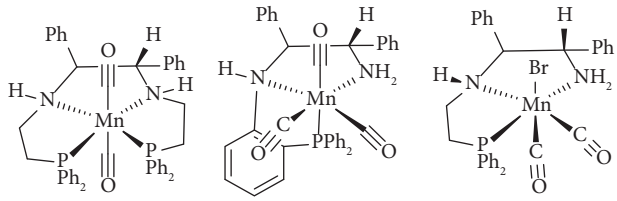

38 39 40

Figure 12: PNNP and PNN pincer complexes.

## 3. Nickel Complexes

Nickel as a catalyst evolved in the 20th century, but its application in TH began to be explored in the late 20th century. Nickel as a catalyst was boosted by studies that showed its potential to catalyze hydrogenation reactions, like the reduction of ketones [78]. Nickel catalyst finds application in synthetic methodologies due to the ease of understanding its catalytic mechanism [21]. This can be demonstrated by nickel nanoparticles, which give outstanding activity in TH reactions compared to traditional catalysis in specific applications, and are also easy to synthesize and reduce a wide range of carbonyls [79].

Ni catalysts can also operate as either homogeneous or heterogeneous catalysts, expanding their applications to sustainable or cost-effective catalytic processes. In heterogeneous systems, the catalyst is immobilized on support systems, which heightens its stability and reusability, making it far better compared to homogeneous [80].

*3.1. Bidentate Ni Complexes.* Several Ni complexes chelated by bidentate ligands have been studied for TH catalysis. For example, the mononuclear and dinuclear complexes **41** and **42** were synthesized from pyrazole derivatives and used for THK (Figure 14) [81]. The monomeric complex **42** exhibited high activity (84% conversion) compared to complex **41** (63% conversion) in the TH of acetophenone using iPrOH and co-catalyst KOH at 82°C. The lower conversion in **41** can be attributed to the steric effect of the two ligands compared to one ligand in complex **42**. Upon testing complex **42** with different bases (KOH, NaOH, $Na_2CO_3$, and $^t$BuOK), the highest conversion was observed with $^t$BuOK, which is consistent with other literature reports that confirm that strong bases give more active catalysts [14]. However, a study by Wang et al. showed NaOH to be superior despite being weaker than $^t$BuOK [82]. Change in electron density on the C=O bond also influenced the catalytic activity of the complex, as seen in Table 5. Castellanos-Blanco has also demonstrated the potential of homogeneous catalysts by using bisphosphine nickel(0) complex **43** to catalyze THK (Figure 14) [78]. This complex gave excellent results of up to 99% yield, addressing a broad substrate scope.

Chiral (pyridyl)imine nickel(II) complexes **44** and **45** (Figure 15) were studied using acetophenone, KOH base, and $^i$PrOH donor and conversions ranging from 54% to 98%, with very low ee (11%–16%), were observed at 82°C for 24 h, with the complex bearing a methyl substituent **44c** (conv 54%) giving lower activity than unsubstituted complex **45a** (conv 84%) [83]. The lower activity in substituted complex **44c** is attributed to reduced electrophilicity in the Ni atom by the more electron-donating methyl group.

Furthermore, the stereochemistry of the complex also influences the catalytic activity. For example, complex **44d** (R-isomer) showed higher activity (98% conversion) than **44c** (S-isomer), because in the S-isomer, there is proximity of the bulkier phenyl group to the nickel atom, which hinders the coordination of the ketone substrate to the metal center. Moreover, investigations of aromatic ketones like 2-methylacetophenone and 2-chloroacetophenone (conversions of 87% and 91%, respectively) revealed that ketones bearing either an EDG or an EWG exhibited lower activities compared to acetophenone (98% conversion). This contradicts Dong et al., who had reported that higher conversions should be observed for substrates bearing EDG or EWG compared to acetophenone [84]. However, the trend in this case is attributed to the steric effect since the substituents in both 2-methylacetophenone and 2-chloroacetophenone are at the ortho position, which is close to the carbonyl center. The mononuclear complex **45** showed higher activity than the dinuclear complexes **44a** and **b** due to less steric hindrance.

The significance of a base in TH reactions was underscored when divalent Ni(II) diphosphine complex **48(a-e)** ($LNiCl_2$) did not yield any activity in the absence of a base (Figure 16) [85]. However, with KOH as the base, in the reduction of acetophenone, 3-nitroacetophenone, or 4-methylacetophenone to the respective alcohols, all the complexes gave similar results, Table 6 at 80°C for 18 h. At low temperature, low conversions were observed due to slow reaction, indicating that the reaction required high activation energy. It was also noted that these complexes were tolerant to other reducible functional groups, like olefinic, as cinnamaldehyde was selectively reduced.

A homogenous nickel-based catalyst **47**, synthesized using 1,2-bis(diisopropylphosphino)ethane ligand and $Ni(COD)_2$ precursor, reduced levulinic acid (LA) to GVL as shown in Scheme 5 [86]. When water was used as a solvent,

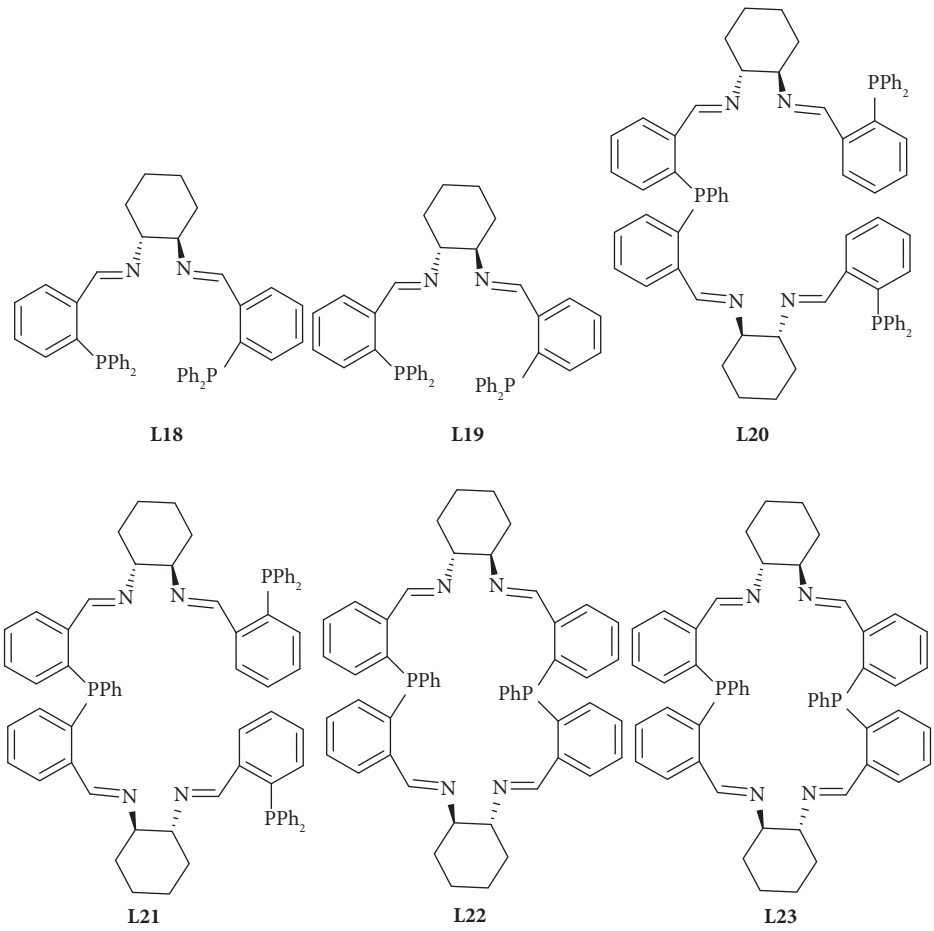


Figure 13: Macrocyclic ligands used for *in situ* catalytic TH of Ketones.

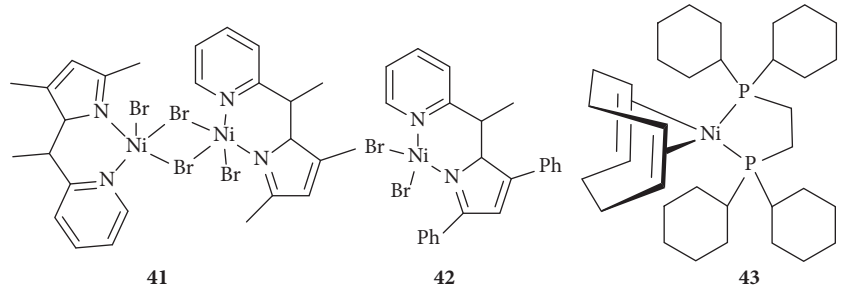


Figure 14: Dinuclear and mononuclear nickel complexes bearing pyrazole ligands and a bisphosphine.

low conversion (20%) was obtained due to the low solubility of both $Ni(COD)_2$ and 1,2-bis(diisopropylphosphino)ethane, but on the addition of THF, conversion increased to 99%. When $Ni(COD)_2$ was used as the catalyst, no conversion was observed, which shows the importance of the dippe ligand in providing the catalytic sites.

Similarly, imino-pyridine complexes **48(a-d)** and **49** were investigated for TH of a variety of ketones, and in the reduction of acetophenone using $^{i}$PrOH donor and KOH base at 80°C for 32 h, moderate conversions of 66%, 72%, 75%, 76%, and 82% were obtained, respectively (Figure 17) [87]. From the kinetic studies, significant conversion was observed within the first 5 h, after which the profile slowed down. This trend is due to the original homogeneous nature of the complex at the start of the reaction and subsequent transformation to Ni(0) nanoparticles. The complex-bearing bulky substituent showed less activity as compared to the less bulky (**48c** methyl substituted [75% conversion], **48a** isopropyl substituent [66% conversion]). This is attributed to high steric effects around the coordination sphere, limiting the coordination of the substrate to the metal center.

In another related study, a four-coordinate 2-hydroxy-1-naphthaldehyde-derived Schiff base nickel complex **50** was synthesized by reacting $NiCl_2$ with €-1-(((2-bromoethyl)

Table 5: The TH of different ketone substrates with complex **42** [81].

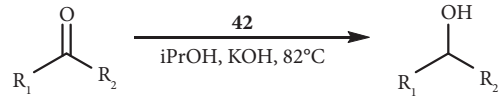


| Substrate | % conversion | TOF ($h^{-1}$) |
|---|---|---|
| 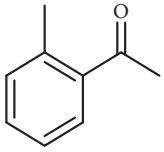 | 78 | 1625 |
| 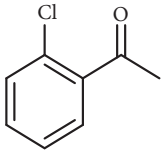 | 88 | 1833 |
| 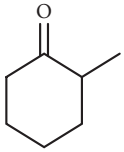 | 51 | 1063 |
| 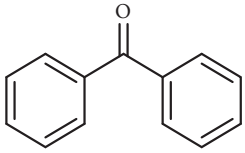 | 72 | 1500 |
| 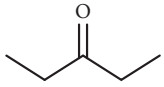 | 35 | 729 |

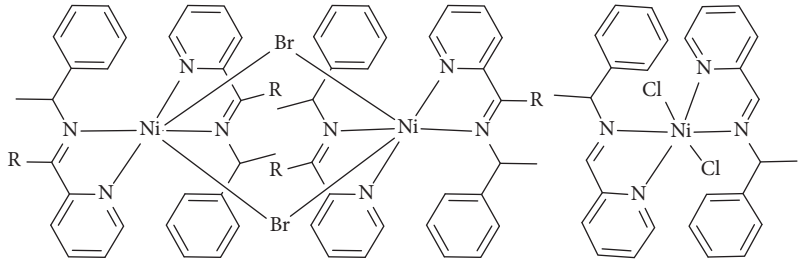


**44a** R=H(S); **44b** R=H(R); **44c** R=Me(S); **44d** R=Me(R) **45**

Figure 15: Dinuclear and mononuclear chiral(pyridyl)imine nickel(II) complexes.

imino)methyl)naphthalen-2-ol [88]. The complex required a base to activate it since it achieved no measurable conversion in the absence of a base. The complex achieved up to 4000 TOF in the reduction of various aromatic ketones at room temperature (Table 7). Generally, it was seen that the steric and electronic properties of the substituent group to the conjugate system containing the reactive ketone bond influenced the reactivity of the ketone and the catalytic performance.

More recently, Song Ma et al. utilized ligands **L24–L29** together with metal precursors $NiCl_2$ and $NiBr_2$ in the reduction of ketones (Figure 18) [89]. Ligands **L24–L28** together with $NiBr_2$ gave yields of up to 43% in the TH of acetophenone using iPrOH donor, KOH base at 130°C for 12 h. Ligand **L29**, remarkably, attained a higher yield (72%) due to the OH substituent group. However, upon replacing $NiBr_2$ with $NiCl_2$, the conversion declined to 52%. Complexes **51a** and **b** were formed by reacting **L29** with $NiBr_2$ and $NiCl_2$, respectively.

Complex **51a** (94%) outperformed **51b** (83% yield) since Cl is less prone to departure compared to Br atoms. Complex **51a** was also used to catalyze the TH of glucose using $^{i}$PrOH donor, and 72% yield was achieved at 130°C after 12 h.

*3.2. Tridentate Ni Complexes.* Ni complexes containing ligands with three donor atoms that bind to the Ni metal ion have been investigated for the TH of ketones. Abubakar et al.

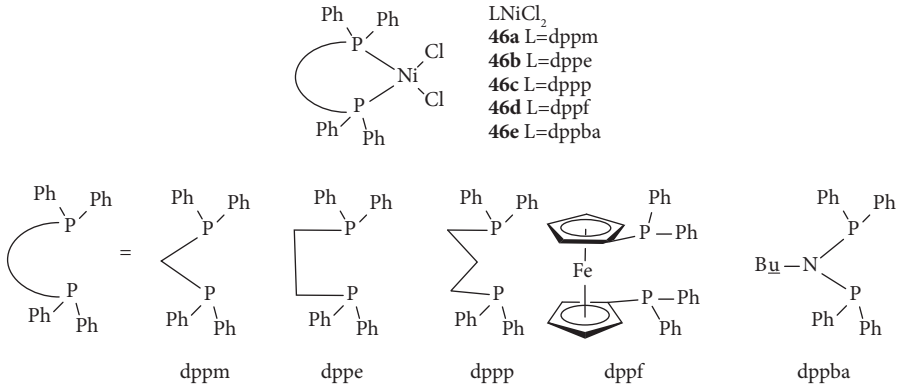


Figure 16: Divalent Ni(II) diphosphine complexes.

Table 6: TH of acetophenone, 3-nitroacetophenone, or 4-methylacetophenone using complex **46** [85].

| Catalyst | %conversion | | |
|---|---|---|---|
| | Acetophenone | 3-Nitro acetophenone | 4-Methyl acetophenone |
| [(dppm)$NiCl_2$] | 97 | 90 | 85 |
| [(dppe)$NiCl_2$] | 97 | 94 | 89 |
| [(dppp)$NiCl_2$] | 96 | 89 | 92 |
| [(dppf)$NiCl_2$] | 97 | 93 | 88 |
| [(dppba)$NiCl_2$] | 95 | 88 | 90 |

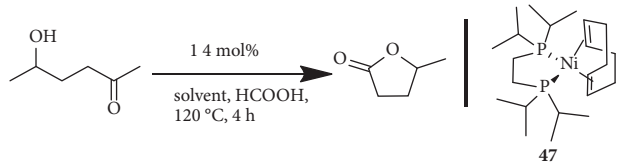


Scheme 5: Catalytic TH of LA to GVL using complex **47** [86].

synthesized the first trinuclear Ni(II) complex **52** using a SB/NHC ligand framework, which was soluble in methanol but insoluble in acetone and chlorinated solvents (Figure 19) [90]. In the TH of acetophenone, the catalyst was found to be base-dependent, as no conversion occurred in a base-free reaction. The co-catalysts KOH and NaOH showed the highest conversion of 90% and 89%, respectively, compared to the organic bases $^t$BuOK (42%) and $Et_3N$ (0%). Aromatic ketones were reduced with conversions of up to 100% after 3h. Cyclic aliphatic ketones yielded 95% for cyclohexanone, 65% for 2-methyl-cyclohexanone, and 82% for 4-methylcyclohexanone. This trend is due to steric hindrance and electronic deactivation properties caused by the substituents, underscoring the role of ligand design in influencing catalytic activity and product yield. Indeed, it has been established that incorporation of chiral ligands enhances enantioselectivity of nickel complexes [91], as illustrated by the incorporation of planar chiral 2.2-paracyclophane-based oxazole-pyrimidine in Ni complex, which achieved up to 99% yield with 98% ee in TH of α,β-unsaturated ketones [92].

DFT has also been utilized to elucidate the mechanistic pathway in THK using nickel as a catalyst [31]. The report shows that nickel facilitates hydrogen transfer by forming hydride intermediates. This information has led to the formation of complexes with high activity and selectivity, like pincer complexes. Qui et al. synthesized SCS nickel pincer complex **53** to reduce 1-acetonaphthone to (R)-(+)-1-(2-naphthyl)ethanol as shown in Scheme 6 [93]. This system used (R)-(+)-1-phenylethanol as a hydrogen donor, and there was high activity due to the π–π stacking effect of the catalyst and donor stabilizing the intermediate and reducing activation energy.

Wang et al. also synthesized nickel pincer complexes **54(a and b)** and **55(a** and **b)** using CNN ligands, which exhibited 99%, 88%, 92%, and 81% yields, respectively, in the reduction of acetophenone using isopropanol donor and NaO$^t$Bu base after 48 h of reaction at 80°C (Figure 20) [94]. This work shows the correlation between nickel complexes' ligand design and catalytic activity.

Another base-dependent system consisting of a bifunctional nickel complex **56** was synthesized using aminophosphinite ligands starting with 3-hydroxybenzaldehyde, Scheme 7 [95]. The complex showed high activity for TH as it reduced acetophenone to 1-phenylethanol with 91% conversion using iPrOH donor, 10 mol% $^t$BuOK, and 5 mol% A at 80°C after 5 h. Increasing the temperature to 100°C resulted in higher conversion (92%) in less than 5h. The catalyst showed no effect in a base-free reaction, and lowering the amount of base led to

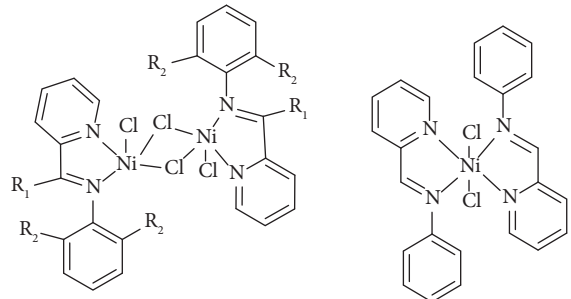

**48a** ($R_1$=H, $R_2$=iPr); **48b** ($R_1$=$CH_3$, $R_2$=iPr)
**48c** ($R_1$=H, $R_2$=$CH_3$); **48d** ($R_1$=$CH_3$, $R_2$=$CH_3$) **49**

Figure 17: Dinuclear and mononuclear imino-pyridine nickel complexes.

Table 7: Results of TH of acetophenone catalyzed by nickel complex **50** bearing 2-hydroxy-1-naphthaldehyde ligands [88].

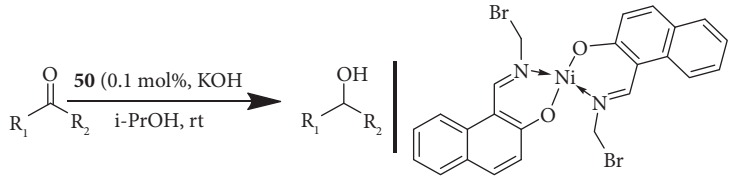

**50**

| Product | Conversion | TON | TOF |
|---|---|---|---|
| 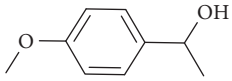 | 100 | 1000 | 4000 |
| 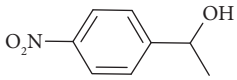 | 99 | 990 | 990 |
| 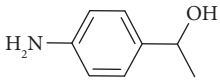 | 100 | 1000 | 4000 |
| 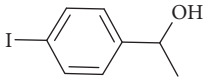 | 100 | 1000 | 4000 |
| 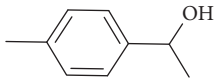 | 87 | 870 | 870 |
| 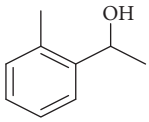 | 84 | 840 | 1680 |
| 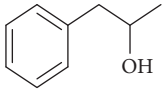 | 91 | 910 | 910 |
| 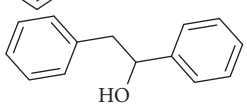 | 100 | 1000 | 1000 |

a decline in conversion. On comparing the reduction of ketones to that of aldehydes, higher conversions were observed for ketones. This is because aldehydes are prone to Adol condensation at the TH conditions. The catalyst tolerated a wide range of functionalities, but for 4-nitroacetophenone, low conversion was observed since the nitro-group poisoned the catalyst. The reaction followed a metal–ligand cooperative mechanism with the intermediacy of an amido $(POCN)Ni^{ii}$ species.

In yet another related study, amido-pincer nickel complexes **57a-b and 58a-d** with oxazolinyl backbones were synthesized from achiral ligands {2-(diethylamino)-N-(2-(4,5-dihydrooxazol-2-yl)phenyl)acetamide, 2-(diethylamino)-N-(2-(4,4-dimethyl-4,5-dihydrooxazol-2-yl)phenyl)-acetamide} and chiral

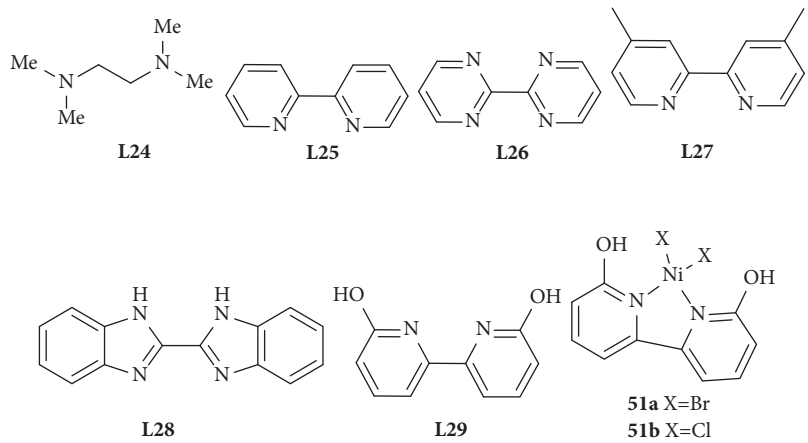


Figure 18: NN ligands coordinated with Ni for THK.

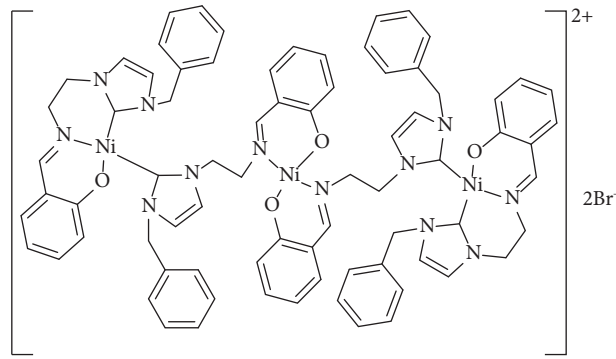


52

Figure 19: Trinuclear nickel complex synthesized using N-heterocyclic carbene ligands.

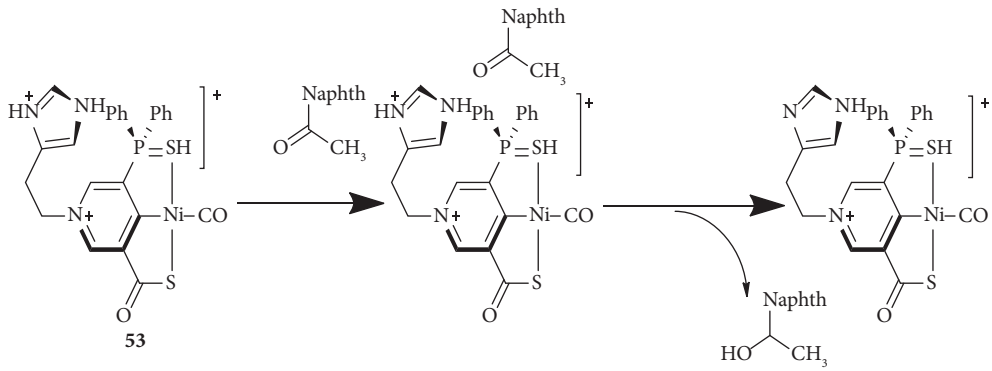


Scheme 6: Reduction of 1-acetonaphthone to (R)-(+)-1-(2-naphthyl) ethanol using complex **53** [93].

ligands {(R)-2-(diethylamino)-N-(2-(4-phenyl-4,5-dihydrooxazol-2-yl)phenyl)acetamide, (R)-N-(2-(4-benzyl-4,5-dihydrooxazol-2-yl)phenyl)-2-(diethylamino)acetamide, (R)-2-(diethylamino)-N-(2-(4-isopropyl-4,5-dihydrooxazol-2-yl)phenyl) acetamide and (R)-2-(diethylamino)-N-(2-(4-isobutyl-4,5-dihydrooxazol-2-yl)phenyl)acetamide}, respectively (Figure 21) [96]. In TH of acetophenone using complex **57a**, $^{i}$PrOH donor at 100°C and a varied amount of KOH base, excess KOH led to undesired product, and a low amount led to incomplete reaction. At temperatures below 100°C, an incomplete reaction was observed. Complex **57b** afforded the lowest yield (35%) compared to the rest due to steric effects. Complexes **58a-d** did not give a stereo alcohol product, which was attributed to low steric crowding around the metal center that was influenced by the involvement of the 6-member nickelacycle with the oxazolinyl ring. These complexes were investigated using a wide

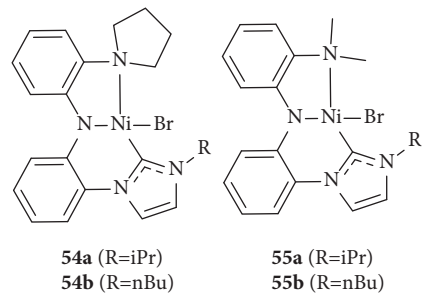

**54a** (R=iPr) **55a** (R=iPr)
**54b** (R=nBu) **55b** (R=nBu)

Figure 20: Nickel complexes bearing unsymmetrical [(carbene)(amino)(amine)]CNN ligands.

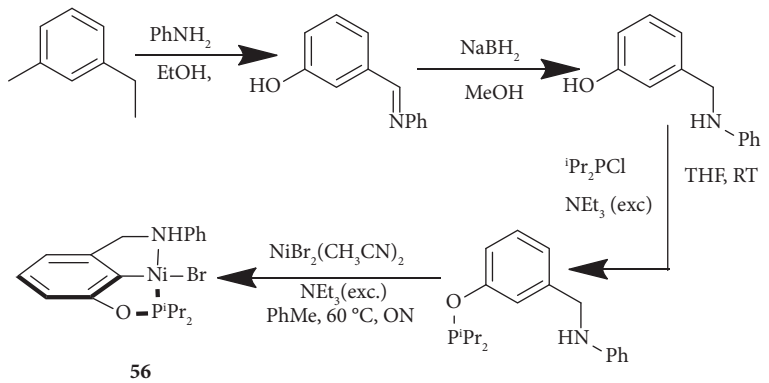

**56**

Scheme 7: Synthesis of a bifunctional nickel complex **56** [95].

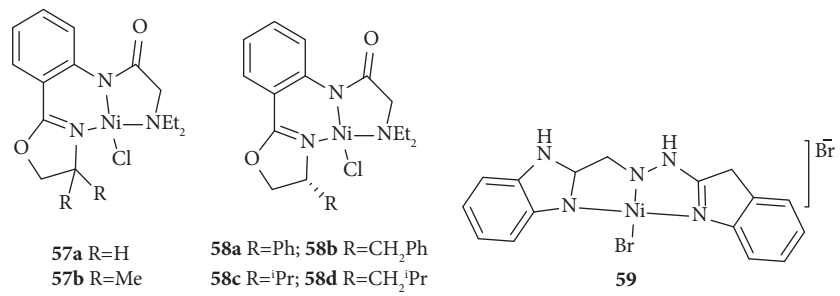

**57a** R=H
**57b** R=Me

**58a** R=Ph; **58b** R=$CH_2Ph$
**58c** R=$^i$Pr; **58d** R=$CH_2{}^i$Pr

**59**

Figure 21: NNN tridentate nickel complexes bearing Amido and benzimidazole ligands.

range of ketones, but were unable to reduce bulky ketones (2-butanones), aliphatic ketones (cyclohexanone), and heteroarene-substituted ketones (3-methyl butan-2-one).

Most recently, nickel complex **59** bearing a benzimidazole-based tri-ligand was used for dual TH of α,β-unsaturated ketones using ammonia borane (AB) (Figure 21) [33]. This complex was synthesized by reacting $NiBr_2$ with benzimidazole ligands. In this study, 1,3-diphenylpro-2-en-1-one was used as the model substrate in the presence of AB in MeOH. This complex showed high conversions, but selectivity was very poor due to cis/trans isomerization and over-reduction Table 8. Using other protic and aprotic solvents (EtOH, THF, CAN, and $H_2O$), methanol afforded the highest conversion. Lowering the amount of AB affected the conversion. There is good conversion at lower temperatures since at high temperatures AB liberates $H_2$ rather than transferring it to the α,β-unsaturated ketones. These complexes reduced the variety of ketones (chalcones, N-heterocycles, S-heterocycles, alkylarenes, and aliphatic substrates) with good yields.

*3.3. Tetradentate Ni Complexes.* Ligands with four donor atoms directly bound to the Ni metal center have also been synthesized and investigated as TH catalysts. For example, air-stable complexes **60–62** were synthesized from the reaction of NiDME and N-heterocyclic ligands at room temperature and used to catalyze THK (Figure 22) [97]. These complexes are soluble in DMSO, acetonitrile, and acetone, insoluble in alcoholic solvents, and partially soluble in chlorinated solvents. Using cyclohexanone as the model substrate, $^i$PrOH donor, and KOH, no reaction proceeded in the absence of a base, and the conversion was very low at lower temperatures. Complex **60** yielded the highest activity (100% conversion after 6h), while **61** and **62** gave 78% and 95%, respectively, after 8 h.

Table 8: TH of α,β-unsaturated acetophenone using tri and tetradentate complex **59** [33].

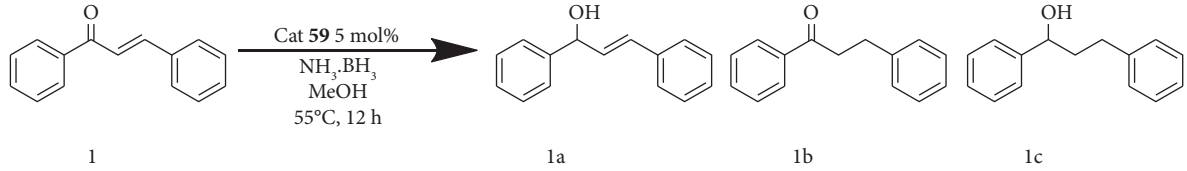


1 1a 1b 1c

| Entry | Cat. (mol%) | Solvent | AB (equiv) | Yield % 1a | Yield % 1b | Yield % 1c |
|---|---|---|---|---|---|---|
| 1 | 1 | MeOH | 2 | 0 | 5 | 95 |
| 2 | 2 | MeOH | 2 | 52 | 0 | 48 |
| 3 | 3 | MeOH | 2 | 48 | 0 | 52 |
| 4 | 4 | MeOH | 2 | 41 | 0 | 59 |
| 5 | 1 | MeOH | 2 | 86 | 0 | 13 |
| 6 | 1 | EtOH | 2 | 0 | 10 | 90 |
| 7 | 1 | THF | 2 | 44 | 7 | 49 |
| 8 | 1 | CAN | 2 | 57 | 5 | 38 |
| 9 | 1 | $H_2O$ | 2 | 34 | 11 | 55 |
| 10 | 1 | MeOH | 1.5 | 0 | 25 | 70 |
| 11 | 1 | MeOH | 1 | 0 | 48 | 37 |

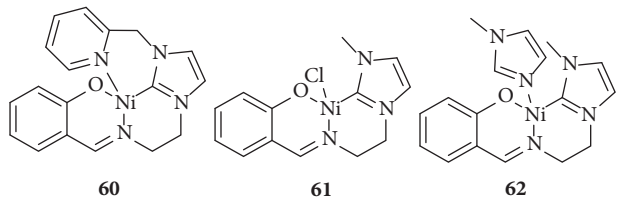

**60** **61** **62**

Figure 22: Nickel complexes bearing N-heterocyclic ligands.

The high yield in **60** and **62** was attributed to the geometrical structure (square planar), which facilitated substrate coordination to the metal center. Complex **60** was used to investigate the effect of the nature of the ketone on the percentage conversion, and it was observed that para-substituted cyclic ketones were easier to reduce than ortho-substituted ones, which was ascribed to the lower steric interactions and stronger electronic effects on the C=O bonds. Furthermore, these complexes showed chemo-selectivity as hex-5-en-2-one and (E)-hex-4-en-2-one were reduced selectively with no product for the C=C bond. A comparative analysis of various studies reveals a trend toward the use of more sustainable and efficient nickel catalysts. For instance, while traditional noble metal catalysts often require high pressures and temperatures, nickel-based systems have shown effectiveness under milder conditions [98]. This is particularly evident in the work of Li et al., who explored the use of a tetradentate nickel complex in asymmetric hydrogenation, achieving high enantioselectivity and conversion rates [99]. Li et al. reduced aromatic ketones using an isopropanol donor, KOH (4 mol%) base, and [NiCl2(PPh3)2] (1 mol%) together with ligand **L30** as the catalyst at 70°C, as shown in Scheme 8**.**

Interestingly, a Ni–Schiff base complex **63** was anchored on an amino-carboxyl functionalized support material (MMAC) containing silica to form an immobilized Ni(II) @MMAC complex (Figure 23) [100]. In the TH of acetophenone studies, it was observed that this catalyst was not temperature-dependent (entries 1–4, Table 9). Usually, high temperature shows adverse effects, indicating that low activation energy is needed, and the reaction is kinetically controlled [39]. This catalyst also demonstrated good yield with different bases (entries 5–9). In the reduction of acetophenone derivatives, little effect was observed for EDG and EWG (benzophenone 87%, 2-bromoacetophenone 94%, 1-(4-methoxyphenyl) ethenone 94%). Comparable results were obtained for homogenous Ni(II)@Schiff base and heterogeneous Ni(II)@MMAC in the TH of acetophenone. The immobilized complex portrayed the advantage of being recycled for up to 10 cycles without losing its activity.

In a similar study by Gupta et al., complexes **64**(**a**-**c**) and **65**(**a**-**c**) were studied as catalysts for TH using 4-chloroacetophenone as the model substrate, together with $^{i}$PrOH donor and KOH base, where these complexes were found active for TH (Figure 24) [101]. It was observed that these complexes require high activation energy, as no conversion was observed at room temperature, but at 60°C, it was 62%, and at 100°C, it was > 90% using complex **64a**. In the absence of a base, no conversion was observed, indicating that the formation of $^{i}$PrOK is crucial in the reaction mechanism. Moreover, it was observed that incorporating co-solvents in the reaction changed the reaction dynamics because nonpolar solvents (toluene and benzene) and weakly coordinating polar solvents (THF and dioxane) gave > 90% conversion, while strong coordinating polar solvents (DMSO and MeCN) and protic solvents (EtOH and MeOH) gave very low and no conversions, respectively. EtOH and

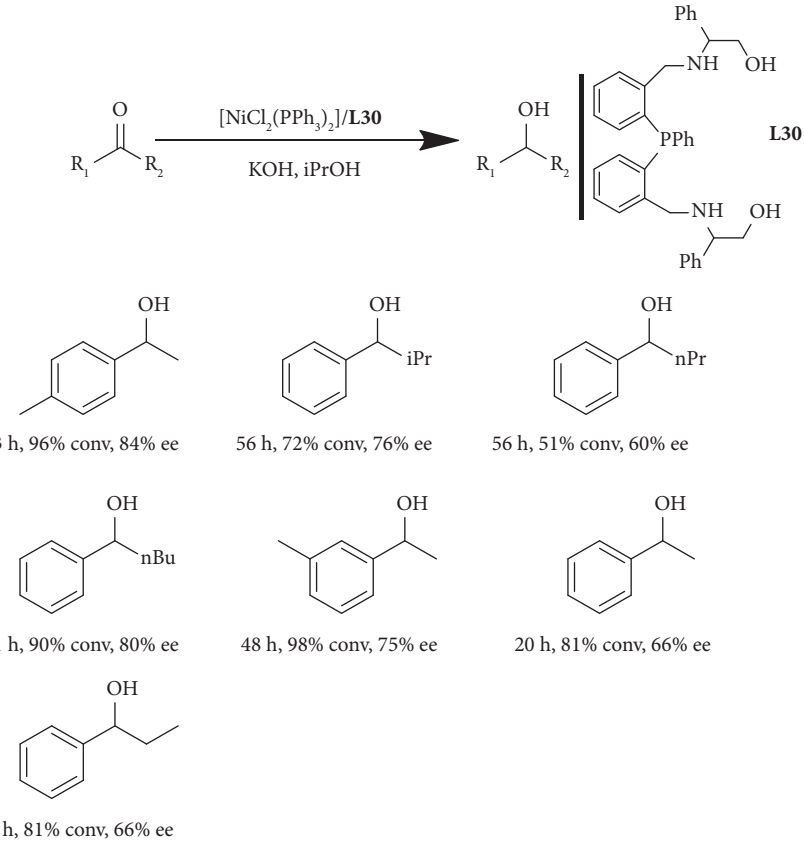


Scheme 8: Selectivity of TH of aromatic ketones using $[NiCl_2(PPh_3)_2]$/**L30** in situ system [99].

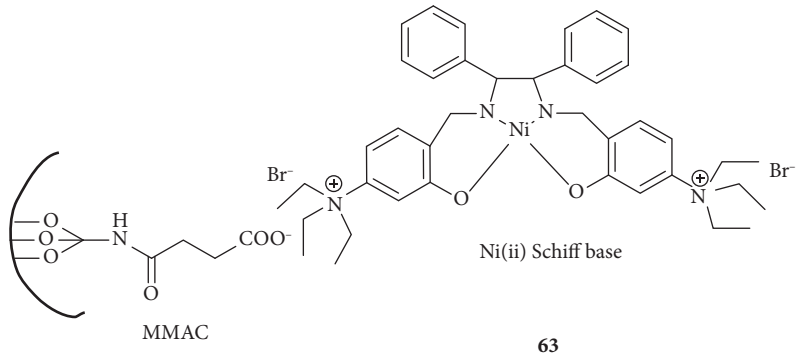


Figure 23: ONNO tetradentate nickel complex immobilized on mesoporous silica.

Table 9: TH of acetophenone catalyzed by Ni(II) Schiff base **63** [100].

| Entry | Temperature (°C) | Base | Yield (%) | Ee (%) |
|---|---|---|---|---|
| 1 | 25 | KOH | 92 | 97 |
| 2 | 40 | KOH | 90 | 75 |
| 3 | 60 | KOH | 85 | 84 |
| 4 | 80 | KOH | 48 | 80 |
| 5 | 25 | KOH | 97 | 98 |
| 6 | 25 | NaOH | 90 | 72 |
| 7 | 25 | $K_2CO_3$ | 95 | 73 |
| 8 | 25 | $K^+(CH_3)_3CO^-$ | 96 | 75.5 |
| 9 | 25 | $Net_3$ | 71 | 60 |

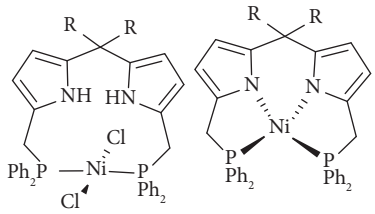

**64a** R=Ph **65a** R=Ph
**64b** R=Et **65b** R=Et
**64c** R=$(CH_2)_5$ **65c** R=$(CH_2)_5$

FIGURE 24: Nickel complexes bearing dipyrromethane–diphosphine ligands.

MeOH lead to the formation of $EtO^-$ or $MeO^-$, which poisons the catalyst. It was further noted that using other donors (EtOH, MeOH, FA/$Net_3$, or ammonium formate) instead of $^i$PrOH did not yield any conversion. Complexes **64a** and **65a**, with a phenyl substituent, outperformed the other complexes having ethyl or cyclohexyl substituted ligands.

Moreover, metallophthalocyanine complexes **66a** and **b**, containing guaiacol and resorcinol groups, were synthesized and applied in CTH of ketones (Figure 25) [102]. The complexes were synthesized by reacting $NiCl_2$ with resorcinol or guaiacol derivatives **L31** and **L32** in the presence of 8-diazabicyclo[5.4.0]undec-7-ene (DBU) and irradiated at 800 W for 20 min. The complexes were found to be soluble in both DMSO and DMF. To study the activity of these complexes in THK, a molar ratio of 10:1:100 for KOH: catalyst:acetophenone was used together with iPrOH donor at 82°C. All the complexes were very active and afforded commendable yields compared to a complex-free reaction (14% conversion). In a base-free reaction using **66b**, no conversion was observed, demonstrating the importance of a base in the formation of a metal alkoxide by substituting a proton from a donor. Under the same conditions, replacing iPrOH with either methanol, ethanol, or HCOOH/$Et_3N$ mixture gave no conversions in all cases after 24 h. Generally, complex **66a**, bearing a guaiacol substituent, was found to be less active compared to **66b**, bearing a resorcinol group. This is because the electron-rich methoxy group in guaiacol reduces the electrophilicity of the metal center due to the inductive effect. More importantly, these complexes exhibited good activity in TH with a wide range of ketones.

Nickel complexes **67** and **68** bearing benzimidazole-based tetradentate ligands were used for dual TH of α,β-unsaturated ketones using AB (Figure 26) [33]. Complex **67** was synthesized by reacting $NiBr_2$ with the benzimidazole ligand, while **68a,b** was obtained by reaction of complex **67** with $NH_4PF_6$ and $NH_4BF_4$, respectively. In the reduction of 1,3-diphenylpro-2-en-1-one in the presence of AB in MeOH, lower conversions were observed (48%, 52%, and 59% yields for **68, 68a,** and **68b,** respectively) compared to their tri-dentate complex **59** (95% yield) counterpart previously reported. The low yields for complexes **67** and **68** can be accounted for by steric crowding, which blocked the substrate from accessing the active sites.

*3.4. Ni Nanoparticles.* The use of nickel nanoparticles has also been explored, as highlighted by Alonso et al., who discussed their role in enhancing reaction rates and selectivity in hydrogen transfer reactions [79]. Alonso performed a base-free THK using NiNPs together with an isopropanol donor, and the remarkable results obtained are shown in Scheme 9. High yields were obtained, which was a result of the large surface area and additional active sites of the NiNPs. NiNPs can be synthesized by reducing nickel salts in the presence of stabilizers like DTBB, decomposing nickel salts in the presence of capping ligands, or decomposing organometallic complexes under hydrogen in the presence of a stabilizing agent [103]. Krishnan et al. also used NiNPs (Ni-NiO/MEM($OT_3$)) catalyst together with isopropanol and decane as the internal standard to reduce 2-cyclohexene-1-one and obtained 73% conversion and > 99% selectivity at 150°C for 48 h [104].

Even more interesting is the stable and easily separable heterogeneous catalyst, magnetic nickel ferrite ($NiFe_2O_4$), explored for THK [105]. In the TH of FUR to FOL using iPrOH donor, a negligible yield was obtained at 180°C without a catalyst, but in the presence of the catalyst, up to 90% yield was observed under the same conditions. Comparing the activity of $NiFe_2O_4$, $CoFe_2O_4$, and $Fe_3O_4$ in TH of FF under the same conditions, $NiFe_2O_4$ afforded the highest conversion (90%) after 4 h. The high conversion by $NiFe_2O_4$ is attributed to its high acid and base amount, as acid–base sites are crucial in CTH. The $NiFe_2O_4$ complex poses an advantage compared to $CoFe_2O_4$ and $Fe_3O_4$ since it does not form Ni(0), which is easily oxidized in air. On studying the effect of the nature of alcohol as a hydrogen source, it was observed that secondary alcohols gave better conversions than primary alcohols (Table 10), which was attributed to the ability of secondary alcohols to possess a sigma-inductive effect [106]. Moreover, due to the magnetic nature of this catalyst, it was easily separated by an external magnetic field and recycled for up to 5 cycles without losing its catalytic activity.

In a related study, Kweon and coworkers synthesized Ni nanoparticles on mesoporous silica nanosphere (Ni@$mSiO_2$) for the TH of ketones [107]. This catalyst was temperature- and base-dependent since no conversion was observed in the absence of base, and the conversion increased as the temperature increased, as seen in Table 11. The catalyst outshone commercial nickel-aluminum alloy in TH due to good thermal stability, uniform pore structure, high surface area, and large pore volume, which was attributed to $mSiO_2$. On recycling the catalyst, it showed lower activity (79% conversion) because metallic Ni was changed (no active sites such as nickel silicide and nickel carbide). The recovered catalyst portrayed a collapsed silica structure and sintered nickel nanoparticles.

Generally, from the foregoing discussion, while both Mn and Ni catalysts have exhibited great potential in TH, as illustrated in Table 12, the superior performance of the Ni-based catalysts in the TH of acetophenone using IPA donor at varying conditions is obvious. Moreover, the catalyst performance is influenced by the nature of the ligand (denticity, donor atom, chirality, and coordination

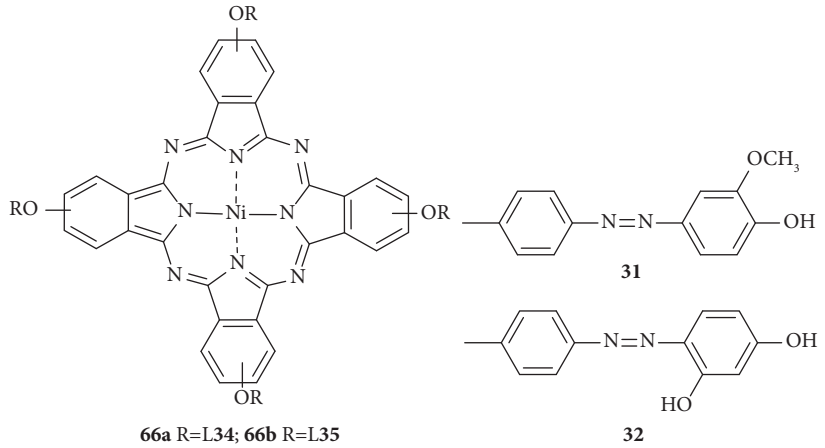


Figure 25: Nickel complexes bearing guaiacol and resorcinol groups, respectively.

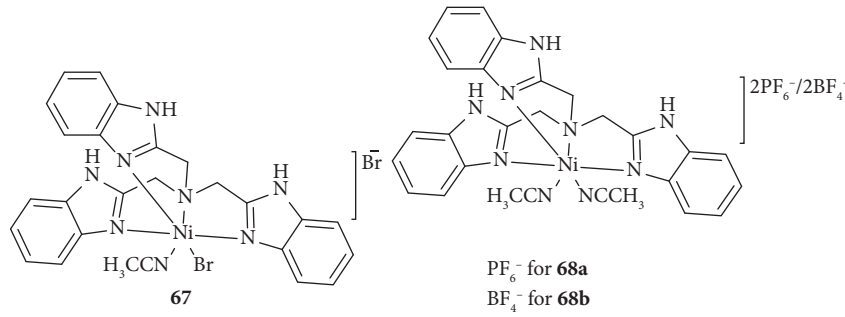


Figure 26: Benzimidazole tetradentate nickel complexes.

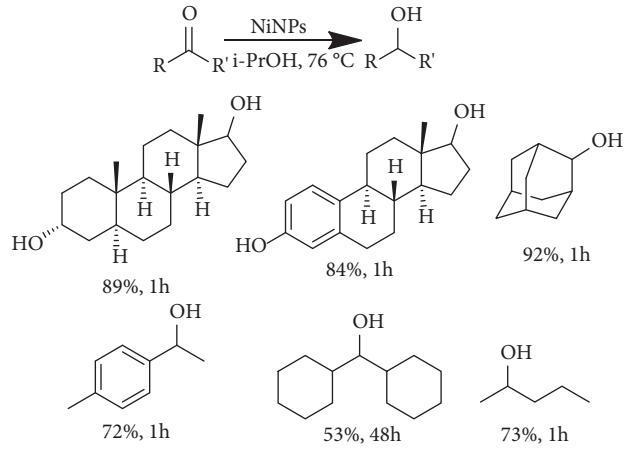


Scheme 9: Base-free transfer hydrogenation of ketone using (Ni-NiO/MEM($OT_3$)) catalyst [79].

Table 10: Effect of hydrogen donors on THK catalyzed by magnetic nickel ferrite [105].

| Donor | Conversion (%) | Yield (%) | Selectivity (%) |
|---|---|---|---|
| Ethanol | 67 | 64 | 96 |
| Isopropanol | 48 | 45 | 94 |
| Isobutanol | 51 | 48 | 64 |
| 2-propanol | 99 | 94 | 95 |
| 2-butanol | 96 | 91 | 95 |
| Tert-butanol | 8 | 2 | 25 |

Table 11: TH of acetophenone catalyzed by Ni nanoparticle (Ni@mSiO$_2$) [107].

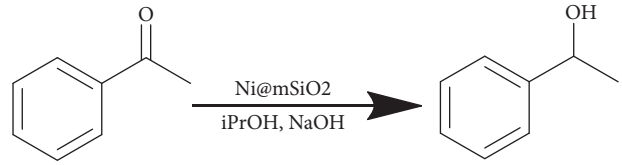


| Catalyst loading | Temperature (°C) | Time min | Base (eq) | Conversion % | Yield % | TON |
|---|---|---|---|---|---|---|
| **1** | 80 | 60 | 1 | – | – | – |
| **1** | 80 | 60 | 1 | 72 | 68 | 68 |
| **1** | 90 | 60 | 1 | 100 | 96 | 96 |
| **1** | 100 | 60 | 1 | 100 | 92 | 92 |
| **1** | 110 | 45 | 1 | 100 | 95 | 95 |

Table 12: Comparative performance of representative Ni and Mn catalysts in the reduction of acetophenone to 1-phenylethanol.

| Entry | Catalyst (mol%) | M | Ligand type | Base | Temp (°C, time h) | Yield % | Conv % | Ee % | TON | TOF ($h^{-1}$) | Ref |
|---|---|---|---|---|---|---|---|---|---|---|---|
| 1. | 3 (0.10) | Mn | NN | $^t$BuOK | 80, 2 | — | > 97 | — | 2000 | 3600 | [66] |
| 2. | 16 (0.02) | Mn | NO | $^t$BuOK | 82, 8 | 79 | — | — | 2633 | 329 | [74] |
| 3. | 42 (1.00) | Ni | NN | $^t$BuOK | 82, 48 | — | 98 | | — | 2042 | [81] |
| 4. | 49 (0.05) | Ni | NN | KOH | 82, 32 | — | 63% | | 126 | — | [87] |
| 5. | 50 (0.10) | Ni | ON | KOH | 25, 6 | — | 83 | — | 4000 | — | [88] |
| 6. | 52 (0.10) | Ni | ONC | KOH | 82, 4 | — | 90 | — | 900 | 230 | [90] |
| 7. | 63 (0.30) | Ni | ONNO | KOH | 25, 16 | 92 | — | 97 | 445 | — | [100] |

geometry), catalyst amount, and reaction conditioning. In addition, the coordination geometry was much influential in determining the reaction mechanism of each complex.

## 4. Conclusion

TH continues to attract attention with the application of greener and hence less hazardous sources of hydrogen such as AB, alcohols, and amines. Despite the advancements made, no universal catalyst exists. TH using nonprecious metal catalysts based on manganese and nickel still faces challenges, chief among which is the development of catalysts with high turnover numbers and selectivity when operating under mild conditions, for a wide range of substrates. Moreover, while there are reports on the use of supported manganese and nickel metal catalysts that allow easy recycling of the catalyst, there is no report yet on the use of these catalysts for industrial processes, a challenge for future research. Enhancing the performance of these metals in TH would require a deeper understanding of the mechanistic pathways and the development of a ligand framework that coordinates well with the metal framework. Nonetheless, the significant findings reported in the last decade concerning TH reactions using manganese and nickel complexes point to a promising future in the field of asymmetric catalysis.

## Data Availability Statement

Data sharing is not applicable to this article as no datasets were generated or analyzed during the current study.

## Conflicts of Interest

The authors declare no conflicts of interest.

## Funding

No funding was received for this manuscript.

## References

[1] Y. Li, S. Lian, J. Wang, and D. Gong, "Bidentate Ru (II)-NC Complexes as Catalysts for Transfer Hydrogenation of Ketones With Ethanol," *Asian Journal of Organic Chemistry* 13, no. 3 (2024): 2193–5807, https://doi.org/10.1002/ajoc.202300496.

[2] A. H. Valekar, M. Lee, J. W. Yoon, et al., "Catalytic Transfer Hydrogenation of Furfural to Furfuryl Alcohol Under Mild Conditions Over Zr-MOFs: Exploring the Role of Metal Node Coordination and Modification," *ACS Catalysis* 10, no. 6 (2020): 3720–3732, https://doi.org/10.1021/acscatal.9b05085.

[3] T. Yang, W. Zhao, H. Li, S. Saravanamurugan, and S. Yang, "Porous Zr-Bibenzyldiphosphonate Nanohybrid With Extra Hydroxy Species for Enhancive Upgrading of Biomass-Based Levulinates," *ChemistrySelect* 3, no. 16 (2018): 4252–4261, https://doi.org/10.1002/slct.201800132.

[4] B. Royo, "Transfer Hydrogenation With Non-Toxic Metals for Drug Synthesis," *RSC Advances* (2018): 105–138.

[5] K. Das, M. K. Barman, and B. Maji, "Advancements in Multifunctional Manganese Complexes for Catalytic Hydrogen Transfer Reactions," *Chemical Communications* 57, no. 69 (2021): 8534–8549, https://doi.org/10.1039/d1cc02512k.

[6] B. Taleb, R. Jahjah, D. Cornu, et al., "Exploring Hydrogen Sources in Catalytic Transfer Hydrogenation: A Review of Unsaturated Compound Reduction," *Molecules* 28, no. 22 (2023): 7541, https://doi.org/10.3390/molecules28227541.

[7] K. Azouzi, D. A. Valyaev, S. Bastin, and J.-B. Sortais, "Manganese—New Prominent Actor in Transfer Hydrogenation Catalysis," *Current Opinion in Green and Sustainable*

*Chemistry* 31 (2021): 100511, https://doi.org/10.1016/j.cogsc.2021.100511.

[8] G. Zhou, A. H. Aboo, C. M. Robertson, et al., "N, O-Vs N, C-Chelation in Half-Sandwich Iridium Complexes: A Dramatic Effect on Enantioselectivity in Asymmetric Transfer Hydrogenation of Ketones," *ACS Catalysis* 8, no. 9 (2018): 8020–8026, https://doi.org/10.1021/acscatal.8b02068.

[9] M. Yaghoubi, I. C. Reyes, and B. J. Stokes, "Pd-Catalyzed Transfer Hydrogenation of Alkenes Using Tetrahydroxydiboron as the Sole Hydrogen Donor," *Synopen* 8, no. 03 (2024): 169–172, https://doi.org/10.1055/a-2367-6943.

[10] X. Hu, G. Wang, C. Qin, et al., "Ligandless Nickel-Catalyzed Transfer Hydrogenation of Alkenes and Alkynes Using Water as the Hydrogen Donor," *Organic Chemistry Frontiers* 6, no. 15 (2019): 2619–2623, https://doi.org/10.1039/c9qo00616h.

[11] F. Foubelo, C. Najera, and M. Yus, "Catalytic Asymmetric Transfer Hydrogenation of Ketones: Recent Advances," *Tetrahedron: Asymmetry* 26, no. 15-16 (2015): 769–790, https://doi.org/10.1016/j.tetasy.2015.06.016.

[12] N. F. Both, J. Fessler, A. Vicenzi, et al., "Air-Stable Manganese NNS Pincer Complexes Enable Ketone Reduction at Room Temperature," *ChemCatChem* 16, no. 9 (2024): E202301562, https://doi.org/10.1002/cctc.202301562.

[13] E. Baráth, "Hydrogen Transfer Reactions of Carbonyls, Alkynes, and Alkenes With Noble Metals in the Presence of Alcohols/ethers and Amines as Hydrogen Donors," *Catalysts* 8, no. 12 (2018): 671, https://doi.org/10.3390/catal8120671.

[14] K. Orosz, G. Papp, Á. Kathó, F. Joó, and H. Horváth, "Strong Solvent Effects on Catalytic Transfer Hydrogenation of Ketones With [Ir (cod)(NHC)(PR3)] Catalysts in 2-Propanol-Water Mixtures," *Catalysts* 10, no. 1 (2019): 17, https://doi.org/10.3390/catal10010017.

[15] R. Ghosh, N. C. Jana, S. Panda, and B. Bagh, "Transfer Hydrogenation of Aldehydes and Ketones in Air With Methanol and Ethanol by an air-Stable Ruthenium–triazole Complex," *ACS Sustainable Chemistry & Engineering* 9, no. 13 (2021): 4903–4914, https://doi.org/10.1021/acssuschemeng.1c00633.

[16] W.-G. Jia, L.-L. Gao, X.-T. Zhi, X.-D. Li, Z.-B. Wang, and Y. Sun, "Half-Sandwich Rhodium Complexes With Phenylene-Based SCS Ligands: Synthesis, Characterization and Catalytic Activities for Transfer Hydrogenation of Ketones," *Polyhedron* 195 (2021): 114978, https://doi.org/10.1016/j.poly.2020.114978.

[17] K. Zhang, S. Okumura, and Y. Uozumi, "Transfer Hydrogenation of Aldehydes and Ketones With Tetrahydroxydiboran in Water by an Amphiphilic Resin-Supported Nano-Palladium Catalyst," *Chemistry Letters* 53, no. 5 (2024): Upae082, https://doi.org/10.1093/chemle/upae082.

[18] S.-H. Ruan, Z.-W. Fan, W.-J. Zhang, et al., "Asymmetric Transfer Hydrogenation of Ketones Catalyzed by Chiral Macrocyclic Cobalt (II) Complexes," *Journal of Catalysis* 418 (2023): 100–109, https://doi.org/10.1016/j.jcat.2023.01.008.

[19] P. Yang, Q. Xia, X. Liu, and Y. Wang, "Catalytic Transfer Hydrogenation/hydrogenolysis of 5-Hydroxymethylfurfural to 2, 5-Dimethylfuran Over Ni-Co/C Catalyst," *Fuel* 187 (2017): 159–166, https://doi.org/10.1016/j.fuel.2016.09.026.

[20] D. Fu, Z. Wang, Q. Liu, S. J. Prettyman, G. A. Solan, and W. H. Sun, "Organometallic Mn (I) Complexes in Asymmetric Catalytic (Transfer) Hydrogenation and Related Transformations," *ChemCatChem* 16, no. 14 (2024): E202301567, https://doi.org/10.1002/cctc.202301567.

[21] M. Sharma, A. M. Perkins, A. K. Duckworth, et al., "Nickel (II) N-Heterocyclic Carbene Complex for the Hydrogenation of 2-Acetylpyridine Under Mild Conditions," *Inorganics* 11, no. 3 (2023): 120, https://doi.org/10.3390/inorganics11030120.

[22] S. Huo, H. Chen, and W. Zuo, "A Cobalt (II) Complex Bearing the Amine (Imine) Diphosphine PN (H) NP Ligand for Asymmetric Transfer Hydrogenation of Ketones," *European Journal of Inorganic Chemistry* 2021, no. 1 (2021): 37–42, https://doi.org/10.1002/ejic.202000826.

[23] S. Huo, Q. Wang, and W. Zuo, "An Iron Variant of the Noyori Hydrogenation Catalyst for the Asymmetric Transfer Hydrogenation of Ketones," *Dalton Transactions* 49, no. 23 (2020): 7959–7967, https://doi.org/10.1039/d0dt01204a.

[24] S. Nath, E. Yadav, A. Raghuvanshi, and A. K. Singh, "Mechanistic Insights and Comparative Analysis of Ru (ii)–NNC Pincer Complexes With Anionic-Protic-And Classical-NHCs for Transfer Hydrogenation of Ketones," *Catalysis Science and Technology* 13, no. 24 (2023): 7085–7099, https://doi.org/10.1039/d3cy01383a.

[25] F. Moniriyan, S. J. Sabounchei, and A. Sedghi, "Synthesis, Characterization and Theoretical Studies of Tris-Cyclometalated Rhodium (III) Complexes: Applications to Asymmetric Transfer Hydrogenation of Ketones," *Journal of Coordination Chemistry* 77, no. 9-10 (2024): 1118–1131, https://doi.org/10.1080/00958972.2024.2355257.

[26] S. Yadav and M. Rao Kuram, "Ir-Catalyzed Transfer Hydrogenation and Alkylation of Aldehydes and Ketones Using Ethanol as the Hydrogen Source," *European Journal of Organic Chemistry* 26, no. 5 (2023): E202201344, https://doi.org/10.1002/ejoc.202201344.

[27] T. V. Roach, M. L. Schmitz, V. A. Leach, M. D. Miller, B. C. Chan, and S. E. Kalman, "Nickel Complexes of Primary Amido-Functionalized N-Heterocyclic Carbene Ligands: Synthesis, Characterization, and Base-Free Transfer Hydrogenation," *Journal of Organometallic Chemistry* 873 (2018): 8–14, https://doi.org/10.1016/j.jorganchem.2018.07.022.

[28] K. Z. Demmans, M. E. Olson, and R. H. Morris, "Asymmetric Transfer Hydrogenation of Ketones With Well-Defined Manganese (I) PNN and Pnnp Complexes," *Organometallics* 37, no. 24 (2018): 4608–4618, https://doi.org/10.1021/acs.organomet.8b00625.

[29] P. Muniyappan, V. Paranthaman, and V. Galmari, "Ru (II) Complexes Containing NOO Donors of Tridentate Schiff Base Ligands: Synthesis, Characterization, Crystal Structure and Catalytic Activity in Transfer Hydrogenation of Ketones," *Chemistry of Inorganic Materials* 1 (2023): 100003, https://doi.org/10.1016/j.cinorg.2023.100003.

[30] A. Gobbo, X. Ma, G. Ciancaleoni, et al., "Ruthenium (II) Tris-Pyrazolylmethane Complexes in Transfer Hydrogenation Reactions," *European Journal of Inorganic Chemistry* 26, no. 18 (2023): E202300078, https://doi.org/10.1002/ejic.202300078.

[31] M. N. Magubane, G. S. Nyamato, S. O. Ojwach, and O. Q. Munro, "Structural, Kinetic, and DFT Studies of the Transfer Hydrogenation of Ketones Mediated by (Pyrazole) Pyridine Iron (II) and Nickel (II) Complexes," *RSC Advances* 6, no. 69 (2016): 65205–65221, https://doi.org/10.1039/c6ra12788f.

[32] J. Yang, L. Yao, Z. Wang, et al., "Manganese (I)-Catalyzed Asymmetric (Transfer) Hydrogenation of Ketones: An Insight Into the Effect of Chiral PNN and NN Ligands," *Journal*

*of Catalysis* 418 (2023): 40–50, https://doi.org/10.1016/j.jcat.2023.01.006.

[33] T. K. Ghosh, A. Sau, D. Mahapatra, and S. Kundu, "Ligand-Modulated Phosphine-Free Ni (II) Complexes for Z-Selective Semi-Transfer Hydrogenation of Alkynes and Dual Transfer Hydrogenation of α, β-Unsaturated Ketones Using Ammonia-Borane," *Organic Chemistry Frontiers* 12, no. 7 (2025): 2321–2331, https://doi.org/10.1039/d4qo02326a.

[34] R. Yu, X. Zhang, F. Hao, et al., "Cobalt-Promoted Transfer Hydrogenation of Azaaryl Ketones by Using Formate as the Hydrogen Source," *European Journal of Organic Chemistry* 26, no. 15 (2023): E202300071, https://doi.org/10.1002/ejoc.202300071.

[35] J. N. Reek, B. de Bruin, S. Pullen, T. J. Mooibroek, A. M. Kluwer, and X. Caumes, "Transition Metal Catalysis Controlled by Hydrogen Bonding in the Second Coordination Sphere," *Chemical Reviews* 122, no. 14 (2022): 12308–12369, https://doi.org/10.1021/acs.chemrev.1c00862.

[36] V. Ritleng and J. G. de Vries, "Ruthenacycles and Iridacycles as Transfer Hydrogenation Catalysts," *Molecules* 26, no. 13 (2021): 4076, https://doi.org/10.3390/molecules26134076.

[37] L. Zhou, D. Liu, H. Lan, et al., "The Origin of Different Driving Forces Between O–H/N–H Functional Groups in Metal Ligand Cooperation: Mechanistic Insight Into Mn (I) Catalysed Transfer Hydrogenation," *Catalysis Science and Technology* 10, no. 1 (2020): 169–179, https://doi.org/10.1039/c9cy02112d.

[38] B. Štefane and F. Požgan, *Asymmetric Hydrogenation and Transfer Hydrogenation of Ketones* (Intech, 2012).

[39] O. R. Onisuru, D. P. Fapojuwo, C. O. Oseghale, O. A. Alimi, and R. Meijboom, "Transfer Hydrogenation of Ketone; an in Situ Approach Toward an eco-Friendly Reduction," *RSC Advances* 12, no. 31 (2022): 19890–19900, https://doi.org/10.1039/d2ra02701a.

[40] S. Abubakar and M. D. Bala, "Transfer Hydrogenation of Ketones Catalyzed by Symmetric Imino-N-Heterocyclic Carbene Co (III) Complexes," *ACS Omega* 5, no. 6 (2020): 2670–2679, https://doi.org/10.1021/acsomega.9b03181.

[41] Q. Liu, M. Liu, J. Chen, J. Wang, and H. Zhou, "Synthesis of Chiral β-Hydroxy Selenides by Ruthenium-Catalysed Transfer Hydrogenation of α-Aryl Selenomethyl Ketones," *Asian Journal of Organic Chemistry* 12, no. 6 (2023): E202300132, https://doi.org/10.1002/ajoc.202300132.

[42] R. T. Kumah and S. O. Ojwach, "Mononuclear and Dinuclear (Pyridyl) Dicarboxamide Ru (II) Hydrido Complexes: Ligand Controlled Coordination Diversity and Catalytic Transfer Hydrogenation of Ketones," *Journal of Organometallic Chemistry* 1005 (2024): 122970, https://doi.org/10.1016/j.jorganchem.2023.122970.

[43] Z. Guo, P. Zhou, L. Jiang, et al., "Electron Localization-Triggered Proton Pumping Toward Cu Single Atoms for Electrochemical CO2 Methanation of Unprecedented Selectivity," *Advanced Materials* 36, no. 14 (2024): 2311149, https://doi.org/10.1002/adma.202311149.

[44] Y. Meng, Y. Jian, J. Li, et al., "Surface-Active Site Engineering: Synergy of Photo-And Supermolecular Catalysis in Hydrogen Transfer Enables Biomass Upgrading and H2 Evolution," *Chemical Engineering Journal* 452 (2023): 139477, https://doi.org/10.1016/j.cej.2022.139477.

[45] M. Wu, L. Bai, F. Deng, J. He, K. Song, and H. Li, "Organic-Inorganic Hybrid Materials for Catalytic Transfer Hydrogenation of Biomass-Derived Carbonyl-Containing Compounds," *Coordination Chemistry Reviews* 523 (2025): 216259, https://doi.org/10.1016/j.ccr.2024.216259.

[46] C. Su, S. Zou, J. Li, L. Wang, and J. Huang, "Supporting Nano Catalysts for the Selective Hydrogenation of Biomass-Derived Compounds," *ChemSusChem* 17, no. 20 (2024): E202400602, https://doi.org/10.1002/cssc.202400602.

[47] H. Li, J. He, A. Riisager, S. Saravanamurugan, B. Song, and S. Yang, "Acid–Base Bifunctional Zirconium N-Alkyltriphosphate Nanohybrid for Hydrogen Transfer of Biomass-Derived Carboxides," *ACS Catalysis* 6, no. 11 (2016): 7722–7727, https://doi.org/10.1021/acscatal.6b02431.

[48] Y. Feng, S. Long, G. Yan, et al., "Manganese Catalyzed Transfer Hydrogenation of Biomass-Derived Aldehydes: Insights to the Catalytic Performance and Mechanism," *Journal of Catalysis* 389 (2020): 157–165, https://doi.org/10.1016/j.jcat.2020.05.037.

[49] B. M. Matsagar, T.-H. Li, C. Van Nguyen, et al., "Furfural Hydrogenation Into Tetrahydrofurfuryl Alcohol Under Ambient Conditions: Role of Ni-Supported Catalysts and Hydrogen Source," *Industrial Crops and Products* 195 (2023): 116390, https://doi.org/10.1016/j.indcrop.2023.116390.

[50] H. Yang, H. Chen, W. Zhou, et al., "Defect Engineered Efficient Catalytic Transfer Hydrogenation of Furfural to Furfuryl Alcohol in Ethanol by Co-Doped LamnO3," *Fuel* 354 (2023): 129388, https://doi.org/10.1016/j.fuel.2023.129388.

[51] J. Qi, Y. Ren, L. Zhang, and X. Hu, "Screening of Ni Based Catalysts Supported on Metal Oxides for Liquid-Phase Hydrogenation of Furfural to Furfuryl Alcohol," *New Journal of Chemistry* 47, no. 36 (2023): 16828–16834, https://doi.org/10.1039/d3nj02140h.

[52] X. Gong, N. Li, Y. Li, and R. Hu, "The Catalytic Hydrogenation of Furfural to 2-Methylfuran Over the Mg-Al Oxides Supported Co-Ni Bimetallic Catalysts," *Molecular Catalysis* 531 (2022): 112651, https://doi.org/10.1016/j.mcat.2022.112651.

[53] C. Gelis, A. Heusler, Z. Nairoukh, and F. Glorius, "Catalytic Transfer Hydrogenation of Arenes and Heteroarenes," *Chemistry--A European Journal* 26, no. 62 (2020): 14090–14094, https://doi.org/10.1002/chem.202002777.

[54] A. Shivhare, A. Kumar, and R. Srivastava, "An Account of the Catalytic Transfer Hydrogenation and Hydrogenolysis of Carbohydrate-Derived Renewable Platform Chemicals Over Non-Precious Heterogeneous Metal Catalysts," *ChemCatChem* 13, no. 1 (2021): 59–80, https://doi.org/10.1002/cctc.202001415.

[55] F. Yang and W. Lai, "Mechanistic Insights Into the Catalytic Transfer Hydrogenation of Furfural to Furfuryl Alcohol Over a N-Doped Carbon-Supported Ni Single Atom Catalyst From First Principles," *New Journal of Chemistry* 47, no. 23 (2023): 11093–11101, https://doi.org/10.1039/d3nj01413d.

[56] D. A. Hey, M. J. Sauer, P. J. Fischer, E. M. H. Esslinger, F. E. Kühn, and W. Baratta, "Acetate Acetylacetonate Ampy Ruthenium (II) Complexes as Efficient Catalysts for Ketone Transfer Hydrogenation," *ChemCatChem* 12, no. 13 (2020): 3537–3544, https://doi.org/10.1002/cctc.202000542.

[57] I. Demianets, V. Cherepakhin, A. Maertens, P. J. Lauridsen, S. M. Sharada, and T. J. Williams, "A New Mechanism of Metal-Ligand Cooperative Catalysis in Transfer Hydrogenation of Ketones," *Polyhedron* 182 (2020): 114508, https://doi.org/10.1016/j.poly.2020.114508.

[58] J. Luo, M. Montag, and D. Milstein, "Metal–Ligand Cooperation With Thiols as Transient Cooperative Ligands: Acceleration and Inhibition Effects in (De) Hydrogenation

Reactions," *Accounts of Chemical Research* 57, no. 12 (2024): 1709–1721, https://doi.org/10.1021/acs.accounts.4c00198.

[59] P. Kisten, S. Vincendeau, E. Manoury, et al., "Understanding Ketone Hydrogenation Catalysis With Anionic Iridium (Iii) Complexes: The Crucial Role of Counterion and Solvation," *Chemical Science* 15, no. 48 (2024): 20478–20492, https://doi.org/10.1039/d4sc04629c.

[60] A. Mandal, K. Ganguli, M. Pradhan, A. Gorai, and S. Kundu, "Selective Transfer Hydrogenation of C= O and Conjugated C= C Bonds Using an Nhc-Based Pincer (CNC) Mni Complex in Methanol," *ChemSusChem* 16, no. 18 (2023): E202300683, https://doi.org/10.1002/cssc.202300683.

[61] S. Yadav, D. Prabha, D. Ahluwalia, A. Bag, and R. Gupta, "Cobalt Complexes as Efficient Cooperative Catalysts for Transfer Hydrogenation," *European Journal of Organic Chemistry* 2022, no. 46 (2022): E202201059, https://doi.org/10.1002/ejoc.202201059.

[62] M. N. Magubane, *Transfer Hydrogenation of Ketones Mediated by (Pyrazolylmethyl) Pyridine Nickel (II) and Iron (II) Complexes* (University of Kwazulu-Natal, 2016).

[63] A. Zirakzadeh, S. R. de Aguiar, B. Stöger, M. Widhalm, and K. Kirchner, "Enantioselective Transfer Hydrogenation of Ketones Catalyzed by a Manganese Complex Containing an Unsymmetrical Chiral PNP′ Tridentate Ligand," *ChemCatChem* 9, no. 10 (2017): 1744–1748, https://doi.org/10.1002/cctc.201700042.

[64] F. Wiedemaier, F. Belaj, and N. C. Mösch-Zanetti, "Elucidating the Role of Amine Donors in Manganese-Catalyzed Transfer Hydrogenation," *Journal of Catalysis* 416 (2022): 103–111, https://doi.org/10.1016/j.jcat.2022.10.020.

[65] B. T. Tsui, M. M. Sung, J. Kinas, F. E. Hahn, and R. H. Morris, "A Ruthenium Protic N-Heterocyclic Carbene Complex as a Precatalyst for the Efficient Transfer Hydrogenation of Aryl Ketones," *Organometallics* 41, no. 15 (2022): 2095–2105, https://doi.org/10.1021/acs.organomet.2c00228.

[66] D. Wang, A. Bruneau-Voisine, and J.-B. Sortais, "Practical (Asymmetric) Transfer Hydrogenation of Ketones Catalyzed by Manganese With (Chiral) Diamines Ligands," *Catalysis Communications* 105 (2018): 31–36, https://doi.org/10.1016/j.catcom.2017.10.028.

[67] A. Bruneau-Voisine, D. Wang, V. Dorcet, T. Roisnel, C. Darcel, and J.-B. Sortais, "Transfer Hydrogenation of Carbonyl Derivatives Catalyzed by an Inexpensive Phosphine-Free Manganese Precatalyst," *Organic Letters* 19, no. 13 (2017): 3656–3659, https://doi.org/10.1021/acs.orglett.7b01657.

[68] K. Ganguli, S. Shee, D. Panja, and S. Kundu, "Cooperative Mn (I)-Complex Catalyzed Transfer Hydrogenation of Ketones and Imines," *Dalton Transactions* 48, no. 21 (2019): 7358–7366, https://doi.org/10.1039/c8dt05001e.

[69] D. Abhishek, S. Wahidur, R. R. Rahaman, and J. R. Fayzullin, "Transfer Hydrogenation of Carbonyl Groups, Imines and N-Heterocycles Catalyzed by Simple, Bipyridine-Based Mn I Complexes," *ChemCatChem* 11, no. 16 (2019): 3844–3852, https://doi.org/10.1002/cctc.201900358.

[70] O. Martínez-Ferraté, C. Werlé, G. Francio, and W. Leitner, "Aminotriazole Mn (I) Complexes as Effective Catalysts for Transfer Hydrogenation of Ketones," *ChemCatChem* 10, no. 20 (2018): 4514–4518, https://doi.org/10.1002/cctc.201800953.

[71] L. Wang, J. Lin, Q. Sun, C. Xia, and W. Sun, "Amino Acid Derived Chiral Aminobenzimidazole Manganese Catalysts for Asymmetric Transfer Hydrogenation of Ketones," *ACS Catalysis* 11, no. 13 (2021): 8033–8041, https://doi.org/10.1021/acscatal.1c00616.

[72] W. Wang, R. Tachibana, Z. Zou, et al., "Manganese Transfer Hydrogenases Based on the Biotin-Streptavidin Technology," *Angewandte Chemie* 135, no. 43 (2023): E202311896, https://doi.org/10.1002/ange.202311896.

[73] R. T. Kumah, F. K. Migwi, M. Schmitz, W. R. Thiel, and S. O. Ojwach, "Novel Metallomacrocyclic Carboxamide Mn (II) Complexes as Efficient Catalysts for the Transfer Hydrogenation of Ketones," *ChemCatChem* 15, no. 23 (2023): E202300971, https://doi.org/10.1002/cctc.202300971.

[74] M. Perez, S. Elangovan, A. Spannenberg, K. Junge, and M. Beller, "Molecularly Defined Manganese Pincer Complexes for Selective Transfer Hydrogenation of Ketones," *ChemSusChem* 10, no. 1 (2017): 83–86, https://doi.org/10.1002/cssc.201601057.

[75] K. Azouzi, A. Bruneau-Voisine, L. Vendier, J.-B. Sortais, and S. Bastin, "Asymmetric Transfer Hydrogenation of Ketones Promoted by Manganese (I) Pre-Catalysts Supported by Bidentate Aminophosphines," *Catalysis Communications* 142 (2020): 106040, https://doi.org/10.1016/j.catcom.2020.106040.

[76] M. A. Mohite, S. Sheokand, D. Mondal, and M. S. Balakrishna, "Catalytic Utility of PNN-Based Mn I Pincer Complexes in the Synthesis of Quinolines and Transfer Hydrogenation of Carbonyl Derivatives," *Dalton Transactions* 53, no. 12 (2024): 5580–5591, https://doi.org/10.1039/d4dt00001c.

[77] G.-Y. Zhang, S.-H. Ruan, Y.-Y. Li, and J.-X. Gao, "Manganese Catalyzed Asymmetric Transfer Hydrogenation of Ketones," *Chinese Chemical Letters* 32, no. 4 (2021): 1415–1418, https://doi.org/10.1016/j.cclet.2020.10.023.

[78] N. Castellanos-Blanco, A. Arévalo, and J. J. García, "Nickel-Catalyzed Transfer Hydrogenation of Ketones Using Ethanol as a Solvent and a Hydrogen Donor," *Dalton Transactions* 45, no. 34 (2016): 13604–13614, https://doi.org/10.1039/c6dt02725c.

[79] F. Alonso, P. Riente, and M. Yus, "Nickel Nanoparticles in Hydrogen Transfer Reactions," *Accounts of Chemical Research* 44, no. 5 (2011): 379–391, https://doi.org/10.1021/ar1001582.

[80] A. K. Bains, A. Biswas, and D. Adhikari, "Nickel-Catalyzed Selective Synthesis of α-Alkylated Ketones via Dehydrogenative Cross-Coupling of Primary and Secondary Alcohols," *Advanced Synthesis & Catalysis* 364, no. 1 (2022): 47–52, https://doi.org/10.1002/adsc.202101077.

[81] M. N. Magubane, M. G. Alam, S. O. Ojwach, and O. Q. Munro, "Orientation Towards Asymmetric Transfer Hydrogenation of Ketones Catalyzed by ((Pyrazolyl) Ethyl) Pyridine Fe (II) and Ni (II) Complexes," *Journal of Molecular Structure* 1135 (2017): 197–201, https://doi.org/10.1016/j.molstruc.2017.01.068.

[82] T. Wang, Y. Xu, M. Du, Z. Hu, and L. Liu, "Synthesis, Characterization and Application of NNN Pincer Manganese Complexes With Pyrazole Framework in α-Alkylation Reaction," *Molecules* 30, no. 7 (2025): 1465, https://doi.org/10.3390/molecules30071465.

[83] R. T. Kumah, N. Tsaulwayo, B. A. Xulu, and S. O. Ojwach, "Structural, Kinetics and Mechanistic Studies of Transfer Hydrogenation of Ketones Catalyzed by Chiral (Pyridyl) Imine Nickel (Ii) Complexes," *Dalton Transactions* 48, no. 36 (2019): 13630–13640, https://doi.org/10.1039/c9dt00024k.

[84] Z. R. Dong, Y. Y. Li, S. L. Yu, G. S. Sun, and J. X. Gao, "Asymmetric Transfer Hydrogenation of Ketones Catalyzed

by Nickel Complex With New PNO-Type Ligands," *Chinese Chemical Letters* 23, no. 5 (2012): 533–536, https://doi.org/10.1016/j.cclet.2012.02.005.

[85] S. Venkatesh, R. R. Panicker, V. Lenin Kumar, et al., "Efficient Catalytic Transfer Hydrogenation Reactions of Carbonyl Compounds by Ni (II)-Diphosphine Complexes," *Journal of Coordination Chemistry* 73, no. 20-22 (2020): 2963–2977, https://doi.org/10.1080/00958972.2020.1837784.

[86] T. Jurado-Vázquez, A. Arévalo, and J. J. García, "Transfer Hydrogenation of Levulinic Acid to γ-Valerolactone and Pyrrolidones Using a Homogeneous Nickel Catalyst," *European Journal of Inorganic Chemistry* 2021, no. 5 (2021): 445–450, https://doi.org/10.1002/ejic.202001063.

[87] N. Tsaulwayo, R. T. Kumah, and S. O. Ojwach, "Applications of Imino-Pyridine Ni (II) Complexes as Catalysts in the Transfer Hydrogenation of Ketones," *Journal of Molecular Structure* 1232 (2021): 129987, https://doi.org/10.1016/j.molstruc.2021.129987.

[88] A. N. Kadafour and M. D. Bala, "Structural Characterization of a Square Planar Ni (II) Complex and Its Application as a Catalyst for the Transfer Hydrogenation of Ketones," *Journal of Coordination Chemistry* 74, no. 17-20 (2022): 2886–2897, https://doi.org/10.1080/00958972.2021.2007890.

[89] S. Ma, X. Wang, J. Cao, H. Chen, Y. Lu, and R. Wang, "Nickel-Catalyzed Efficient Transfer Hydrogenation of Ketones," *ChemistrySelect* 9, no. 19 (2024): E202400730, https://doi.org/10.1002/slct.202400730.

[90] S. Abubakar, H. Ibrahim, and M. D. Bala, "Transfer Hydrogenation of Ketones Catalyzed by a Trinuclear Ni (II) Complex of a Schiff Base Functionalized N-Heterocyclic Carbene Ligand," *Inorganica Chimica Acta* 484 (2019): 276–282, https://doi.org/10.1016/j.ica.2018.09.057.

[91] H. Xu, P. Yang, P. Chuanprasit, H. Hirao, and J. Zhou, "Nickel-Catalyzed Asymmetric Transfer Hydrogenation of Hydrazones and Other Ketimines," *Angewandte Chemie International Edition* 54, no. 17 (2015): 5112–5116, https://doi.org/10.1002/anie.201501018.

[92] J. Wang, Q.-X. Xie, X. Li, C.-B. Yu, and Y.-G. Zhou, "Design and Synthesis of [2.2] Paracyclophane-Based Oxazole-Pyrimidine Ligands and Application in Nickel-Catalyzed 1, 2-Reduction of α, β-Unsaturated Ketones," *Authorea Preprints* (2023).

[93] B. Qiu, W. Wang, and X. Yang, "Computational Design of SCS Nickel Pincer Complexes for the Asymmetric Transfer Hydrogenation of 1-Acetonaphthone," *Catalysts* 9, no. 1 (2019): 101, https://doi.org/10.3390/catal9010101.

[94] Z. Wang, X. Li, S. Xie, T. Zheng, and H. Sun, "Transfer Hydrogenation of Ketones Catalyzed by Nickel Complexes Bearing an NHC [CNN] Pincer Ligand," *Applied Organometallic Chemistry* 33, no. 6 (2019): E4932, https://doi.org/10.1002/aoc.4932.

[95] M. Segizbayev, Ö. Öztopçu, D. Hayrapetyan, D. Shakhman, K. A. Lyssenko, and A. Y. Khalimon, "Transfer Hydrogenation of Aldehydes and Ketones Catalyzed Using an Aminophosphinite Pocn H Pincer Complex of Ni (Ii)," *Dalton Transactions* 49, no. 34 (2020): 11950–11957, https://doi.org/10.1039/d0dt02264k.

[96] R. A. Jagtap, S. B. Ankade, R. G. Gonnade, and B. Punji, "Achiral and Chiral NNN-Pincer Nickel Complexes With Oxazolinyl Backbones: Application in Transfer Hydrogenation of Ketones," *New Journal of Chemistry* 45, no. 27 (2021): 11927–11936, https://doi.org/10.1039/d1nj01698a.

[97] S. Abubakar and M. D. Bala, "Application of Ni (II) Complexes of Air Stable Schiff Base Functionalized N-Heterocyclic Carbene Ligands as Catalysts for the Transfer Hydrogenation of Aliphatic Ketones," *Journal of Coordination Chemistry* 71, no. 16-18 (2018): 2913–2923, https://doi.org/10.1080/00958972.2018.1493199.

[98] B. García, J. Moreno, G. Morales, J. A. Melero, and J. Iglesias, "Production of Sorbitol via Catalytic Transfer Hydrogenation of Glucose," *Applied Sciences* 10, no. 5 (2020): 1843, https://doi.org/10.3390/app10051843.

[99] Y.-Y. Li, S.-L. Yu, W.-Y. Shen, and J.-X. Gao, "Iron-Cobalt-And Nickel-Catalyzed Asymmetric Transfer Hydrogenation and Asymmetric Hydrogenation of Ketones," *Accounts of Chemical Research* 48, no. 9 (2015): 2587–2598, https://doi.org/10.1021/acs.accounts.5b00043.

[100] M. Shukla, K. Barick, H. Salunke, and S. Chandra, "Chiral Salen-Ni (II) Based Spherical Porous Silica as Platform for Asymmetric Transfer Hydrogenation Reaction and Synthesis of Potent Drug Intermediate Montekulast," *Molecular Catalysis* 502 (2021): 111367, https://doi.org/10.1016/j.mcat.2020.111367.

[101] R. Gupta, A. Kumar, and G. Mani, "Dipyrromethane–Diphosphine: The Effect of Meso Substituents on the Formation of Nickel Complexes and on Their Performance in the Transfer Hydrogenation of Ketones," *Dalton Transactions* 52, no. 48 (2023): 18332–18341, https://doi.org/10.1039/d3dt03163b.

[102] U. Işık, M. Namlı, C. Kantar, S. Şaşmaz, and M. Aydemir, "New Metallophthalocyanine (M: Ni (II) and Fe (II)) Complexes as Efficient Catalysts for Transfer Hydrogenation of Various Ketones," *Journal of Organometallic Chemistry* 1020 (2024): 123325, https://doi.org/10.1016/j.jorganchem.2024.123325.

[103] M. R. Hassan, F. Yasmin, F. K. Noor, M. S. Rahman, M. S. Uddin, and S. Bhowmik, "Synthesis and Applications of Nickel Nanoparticles (NiNPs)—Comprehensive Review," *JUC* 19, no. 1 (2023): 9–37, https://doi.org/10.22147/juc/190102.

[104] D. Krishnan, L. Schill, M. R. Axet, K. Philippot, and A. Riisager, "Nanocatalysts Based on Ni Nanoparticles in Functionalized Ionic Liquids for Chemoselective Hydrogenation and Transfer Hydrogenation of A, B-Unsaturated Carbonyl Compounds," *ChemCatChem* 16, no. 4 (2024): E202301441, https://doi.org/10.1002/cctc.202301441.

[105] J. He, S. Yang, and A. Riisager, "Magnetic Nickel Ferrite Nanoparticles as Highly Durable Catalysts for Catalytic Transfer Hydrogenation of Bio-Based Aldehydes," *Catalysis Science and Technology* 8, no. 3 (2018): 790–797, https://doi.org/10.1039/c7cy02197f.

[106] E. Baráth, "Hydrogen Transfer Reactions of Carbonyls, Alkynes, and Alkenes With Noble Metals in the Presence of Alcohols/ethers and Amines as Hydrogen Donors," *Catalysts* 8, no. 12 (2018): 671, https://doi.org/10.3390/catal8120671.

[107] H. Kweon, S. Jang, A. Bereketova, J. C. Park, and K. H. Park, "Highly Dispersed Ni Nanoparticles on Mesoporous Silica Nanospheres by Melt Infiltration for Transfer Hydrogenation of Aryl Ketones," *RSC Advances* 9, no. 25 (2019): 14154–14159, https://doi.org/10.1039/c9ra01608b.